AD_____

AWARD NUMBER: W81XWH-08-1-0455

TITLE: Isolation and Characterization of Prostate Cancer Stem Cells

PRINCIPAL INVESTIGATOR: Isla Garraway, M.D., Ph.D.

CONTRACTING ORGANIZATION: University of California, Los Angeles
    Los   Angeles, CA 90095

REPORT DATE: August 2009

TYPE OF REPORT: Annual Summary

PREPARED FOR: U.S. Army Medical Research and Materiel Command
                Fort Detrick, Maryland 21702-5012

DISTRIBUTION STATEMENT: Approved for Public Release;
                Distribution Unlimited

The views, opinions and/or findings contained in this report are those of the author(s) and
should not be construed as an official Department of the Army position, policy or decision
unless so designated by other documentation.

REPORT DOCUMENTATION PAGE

Form Approved
OMB No. 0704-0188

Public reporting burden for this collection of information is estimated to average 1 hour per response, including the time for reviewing instructions, searching existing data sources, gathering and maintaining the data needed, and completing and reviewing this collection of information. Send comments regarding this burden estimate or any other aspect of this collection of information, including suggestions for reducing this burden to Department of Defense, Washington Headquarters Services, Directorate for Information Operations and Reports (0704-0188), 1215 Jefferson Davis Highway, Suite 1204, Arlington, VA 22202-4302. Respondents should be aware that notwithstanding any other provision of law, no person shall be subject to any penalty for failing to comply with a collection of information if it does not display a currently valid OMB control number. **PLEASE DO NOT RETURN YOUR FORM TO THE ABOVE ADDRESS.**

1. REPORT DATE	2. REPORT TYPE	3. DATES COVERED
1 August 2009	Annual Summary	1 Aug 2008 – 31 Jul 2009

4. TITLE AND SUBTITLE	5a. CONTRACT NUMBER
Isolation and Characterization of Prostate Cancer Stem Cells	
	5b. GRANT NUMBER
	W81XWH-08-1-0455
	5c. PROGRAM ELEMENT NUMBER

6. AUTHOR(S)	5d. PROJECT NUMBER
Isla Garraway, M.D., Ph.D.	
	5e. TASK NUMBER
E-Mail: igarraway@mednet.ucla.edu	5f. WORK UNIT NUMBER

7. PERFORMING ORGANIZATION NAME(S) AND ADDRESS(ES)	8. PERFORMING ORGANIZATION REPORT NUMBER
University of California, Los Angeles Los Angeles, CA 90095	

9. SPONSORING / MONITORING AGENCY NAME(S) AND ADDRESS(ES)	10. SPONSOR/MONITOR'S ACRONYM(S)
U.S. Army Medical Research and Materiel Command Fort Detrick, Maryland 21702-5012	
	11. SPONSOR/MONITOR'S REPORT NUMBER(S)

12. DISTRIBUTION / AVAILABILITY STATEMENT
Approved for Public Release; Distribution Unlimited

13. SUPPLEMENTARY NOTES

14. ABSTRACT

Cells derived from various organs and tumors that exhibit sphere-like growth in vitro include stem and early progenitors. Therefore, human prostate epithelial cells that can develop into "prostaspheres" may allow enrichment and characterization of these rare cell types. We have generated an extensive collection of prostaspheres, derived from normal and cancerous prostate specimens from patients undergoing urologic surgery at UCLA Medical Center. These prostaspheres have been evaluated for the functional abilities to self-renew and differentiate into the full complement of prostate epithelial cell types. In addition to interrogating stem-cell qualities, we evaluated whether normal and cancer prostaspheres could be distinguished. To do this, we performed FISH analysis on paraffin-embedded prostaspheres with probes detecting the TMPRSS-ERG translocation that has been described in the majority of human prostate cancers. We found that although approximately 70% of the prostate cancer specimens in our collection displayed the TMPRSS-ERG rearrangement, it was not present in the prostaspheres. The aims of our project are to define factors that enable prostate cancer cells containing the TMPRSS-ERG translocation to be isolated and maintained in vitro and in vivo so that cancer stem/progenitor populations can be characterized and interrogated.

15. SUBJECT TERMS
Prostate Cancer, prostate stem cells, TMPRSS-ERG, prostate xenografts

16. SECURITY CLASSIFICATION OF:			17. LIMITATION OF ABSTRACT	18. NUMBER OF PAGES	19a. NAME OF RESPONSIBLE PERSON USAMRMC
a. REPORT	b. ABSTRACT	c. THIS PAGE			
U	U	U	UU	76	19b. TELEPHONE NUMBER *(include area code)*

Standard Form 298 (Rev. 8-98)
Prescribed by ANSI Std. Z39.18

Table of Contents

I - INTRODUCTION:

As a new faculty in the UCLA Department of Urology, I was awarded a seed grant from the Department of Defense in 2006 to support preliminary work on human prostate cancer stem cells. This project rapidly progressed under the mentorship of Dr. Owen Witte with three completed manuscripts ((1),Garraway et al, *in press*, Goldstein et al, *submitted*, see appendix). The aims of this proposal are based on the most profound and surprising observation from our initial study. We discovered that prostate stem/early progenitor cells that form spheres in vitro, lack the TMPRSS-ERG translocation found in the original tumor. None of the prostaspheres generated from 10 different TMPRSS-ERG+ tumors contained this fusion when examined by fluorescence in situ hybridization (FISH). Our findings suggest either ETS rearrangements are not present at the stem/progenitor cell level, or that genetically deranged prostate cells are particularly vulnerable to apoptosis or senescence in vitro. We are currently requesting support to pursue in depth evaluation of the growth requirements that enable survival and expansion of prostate stem/progenitor cells that contain ETS rearrangements, if they exist. Generating an extensive collection of human prostate cancer stem cells would provide valuable biological tools for understanding the mechanisms of tumorigenesis and developing new therapeutic targets. Our approach is in line with the DOD's mission to support research with high impact potential.

II - BODY:

Background and Specific Aims:

Expansion of Prostate Stem/Progenitor Cells: The study of prostate stem cells (SCs) is challenging since these highly specialized cells capable of both self-renewal and differentiation are so rare. It is estimated that less than 1% of prostate basal cells are SCs(2, 3). One method that enables expansion of the stem/early progenitor compartment in other organ systems is culturing dissociated primary cells as spheres(4, 5). Spheres are multicellular globes that form in anchorage-independent conditions, and these cultures have been commonly used to study mammary and nervous system development(6, 7). In such studies, spheres can be dissociated and passaged for multiple generations (self-renew), as well as be induced to form fully differentiated progeny.

Reproducible models of normal and deranged prostate development would be valuable for deciphering tumorigenesis and developing new therapeutic approaches. We observed robust formation of prostaspheres in 3D-Matrigel cultures seeded with cells obtained from dissociated prostate surgical specimens (Garraway et al. unpublished results). Our prostasphere collection was derived from tissue representing the complete spectrum of benign and malignant prostate glands. Similar to previously described sphere systems, prostaspheres demonstrated clonal growth and self-renewal(8, 9). With long-term culture in Matrigel, branching of spheres with expression of mature (luminal) markers was observed in a subset of cells.

The TMPRSS-ERG Fusion is Not Identified in Prostaspheres: Since prostaspheres were generated from primary tumors, we presumed that in vitro cultures would include clonally derived benign and cancerous prostaspheres, reflective of the heterogeneity of glands found in tissue specimens. We were not able, however, to distinguish prostaspheres based on phenotype, marker expression, or growth rate. With the discovery of prevalent gene rearrangements involving ETS family members in prostate cancer, we anticipated that cytogenetic tools may enable identification of cancerous prostaspheres(10). Gene fusions involving ERG, ETV1, and ETV4 involve a variety of 5' partners that direct aberrant expression of these transcription factors and possibly initiate a cascade of events leading to tumorigenesis (10). The most common rearrangement involves juxtaposition of the androgen-regulated TMPRSS2 gene with ERG. TMPRSS-ERG gene fusions have been detected in primary prostate tumor specimens, metastases, and xenografts by fluorescence in situ hybridization (FISH)(10). Analysis of prostate tumor surgical cohorts have found 36-78% of prostate cancers possess the TMPRSS-ERG fusion(10). We wondered whether we could use TMPRSS-ERG to distinguish normal and malignant prostaspheres. The presence of this fusion in individual prostaspheres may suggest that cancer stem/early progenitor cells can be expanded in our cultures.

To test the feasibility of this approach, FISH analysis was performed on select prostate tissue specimens and coordinating prostaspheres (Garraway et al, unpublished results). The TMPRSS-ERG fusion was found in approximately 60% of cancer cases tested. Surprisingly, the fusion was conspicuously absent from prostasphere cultures derived from TMPRSS-ERG+ tissues, even when the specimens contained >90% tumor. Analysis of monolayer cultures concomitantly derived from prostate tumor specimens also failed to demonstrate the presence of the gene fusion, indicating that both spheroid and adherent cultures select for fusion-negative cells.

Review of ETS Rearrangements in Cultured Prostate Epithelial Cells: The TMPRSS-ERG fusion has previously been identified in only one prostate cancer cell line, NCI-H660, derived from an androgen-independent small cell carcinoma of the prostate(11, 12). None of the common prostate cancer cell lines including LnCaP, DU-145, PC-3,

and CWR22 contain this fusion(10). LnCaP and MDA-PCa2b were recently reported to contain rearrangement of the ETV1 gene to a prostate specific region resulting in aberrant expression with increased invasive activity(10). The general inability to culture primary prostate cells that contain TMRPSS-ERG, and the under-representation of ETS rearrangements in prostate cancer cell lines is intriguing and suggests critical elements are absent in vitro, preventing the growth of these cells.

We have formulated three distinct possibilities why TMPRSS-ERG is not preserved in human prostate cells in vitro 1) prostate cancer stem cells responsible for propagating primary cells do not contain the TMPRSS-ERG fusion, rather it is a genetic event that occurs later in tumorigenesis as a result of genomic instability 2) Fusion-positive prostate cells undergo anoikis, apoptosis, or senescence unless additional growth/survival factors or stromal interaction is provided, or 3) genetically normal cells have a dramatic growth advantage over TMPRSS-ERG cancer cells, resulting in their rapid overgrowth.

Since the TMPRSS-ERG fusion is so prevalent in prostate cancer regardless of grade or stage, analyses of the genetic impact of these rearrangements is critical. Deciphering the fundamental survival factors necessary for culturing these cells will yield biological tools for the study of ETS rearrangements in addition to valuable insight into the vulnerabilities of these cells. Consequently, we proposed to define what factors are critical for survival and expansion of TMPRSS-ERG fusion-positive prostate cancer cells via the following aims:

Aim 1: Generate a collection of tumor specimens that contain the TMPRSS-ERG translocation, as demonstrated by FISH of the primary tumor.
   a. Generate xenografts from TMPRSS-ERG tissue specimens
   b. Generate prostasphere and monolayer (adherent) cultures from TMPRSS-ERG specimens in a variety of culture conditions, including altering media and additives (i.e., androgen, stroma)
   c. Generate stocks of cryopreserved dissociated prostate cells from TMPRSS-ERG specimens

Aim 2: Assess for the retention of the TMPRSS-ERG mutation in xenografts, expanded in vitro monolayer (adherent) cultures, and prostasphere cultures.

Aim 3: Assess the effect of inhibiting anoikis and/or apoptosis pathways in dissociated prostate epithelial cells derived from TMPRSS-ERG+ tissues on prostasphere formation via viral mediated gene transfer of genes that are known to disrupt these processes (i.e., Bcl-2, Ras, dominant negative p53).

<u>Preliminary Data:</u>

Development of Self-Renewing Human Prostaspheres: We generated spheres from prostate tissue specimens of 35 patients undergoing cancer surgery. Prostaspheres developed indiscriminately from all tissue types, regardless of Gleason grade, with 1 to 4% of unfractionated cells capable of sphere formation. Variability in the efficiency of prostasphere development was observed among samples but did not appear to be associated with any patient clinical or pathological characteristics (see appendix Garraway et al., in press) To assess the self-renewal potential of human prostaspheres, dissociation of the spheres into single cell suspensions were performed followed by re-plating in Matrigel. New spheres were observed in independent experiments with a variety of patient specimens for more than 16 generations (data not shown). Prostaspheres that were culture for >2 weeks in Matrigel and/or cultured with 10-7nM testosterone formed branching structures, demonstrating differentiation capability (see appendix Garraway et al., in press).

Prostaspheres Express Basal Markers: The prostate epithelium is composed of basal cells, including stem cells and transient amplifying cells, terminally differentiated luminal cells, and neuroendocrine cells(13). Prostate epithelial cells can be differentiated based on expression of a variety of markers(14). The basal markers CK5, alpha 6 integrin (CD49f), CD44, and p63 were strongly expressed by the majority of sphere-forming cells (see appendix Garraway et al., in press). On the other hand, luminal markers, including AR (androgen receptor) and PSA (prostate-specific antigen) were not observed in prostaspheres cultured in the absence of androgen. CK8, a marker expressed in intermediate and luminal cells, was occasionally noted in sphere-forming cells. In these CK8+ cells, co-expression with CK5 was also demonstrated. Expression of the neuroendocrine marker, synaptophysin was not observed (data not shown). Taken together, the pattern of expression of sphere-forming cells most closely resembles normal basal cells; with predominately CK5, CD44, alpha integrin (CD49f), and p63 expression.

TMPRSS-ERG Expression in Primary Prostate Tumors and Prostaspheres: The TMPRSS-ERG fusion represents a specific genetic marker for prostate cancer. We opted to take advantage of this trait in order to assess whether prostaspheres derived from TMPRSS-ERG+ tissues retained this marker. FISH was performed on paraffin embedded tumors and coordinating prostaspheres. Although the fusion was readily found in a substantial proportion of prostate tumor specimens, it was not identified in any of the prostaspheres (Garraway et al., in press). So far, we have analyzed

prostaspheres from 10 fusion-positive primary tissue specimens. Additionally, we have tested prostate epithelial cells derived from a subset of the fusion+ tissues that were grown as an adherent monolayer. All of these in vitro cultures were also negative for the TMPRSS-ERG fusion by FISH.

Conclusions from Preliminary Data: We found that a small subset of epithelial cells obtained from a wide variety of dissociated human prostate specimens form prostaspheres that possess features of self-renewal and branching morphogenesis, suggestive of stem/progenitor activity in these cultures. Prostaspheres can be dissociated, passaged, and cryopreserved with the retention of sphere-forming ability. These practical attributes of human prostaspheres could facilitate high-throughput studies of stem/progenitor cells generated from large collections of patient specimens. However, the lack of the TMPRSS-ERG fusion in prostaspheres derived from tumors containing this translocation indicates that prostaspheres may only form from normal cells. The TMPRSS-ERG cancer stem cells either do not exist, or lack fundamental survival traits that normal stem cells possess. The aims detailed below will attempt to provide data that may answers the questions related to the culture of TMPRSS-ERG prostate cancer cells.

III -KEY RESEARCH ACCOMPLISHMENTS:

The tasks of the training program include:

1) Regularly meet with mentor to discuss career goals and progress
2) Attend group meetings, journal clubs, and seminars related to research topics
3) Direct research project outlined in the proposal according to the specific aims:
   a. Develop a collection of TMPRSS-ERG fusion positive human prostate cancers
   b. Evaluate the ability to preserve the TMPRSS-ERG fusion in prostaspheres by varying culture conditions.
   c. Evaluate the ability to propagate TMPRSS-ERG+ cells in prostate epithelial monolayer cultures and in xenografts
   d. Perform viral mediated gene transfer of genes that block anoikis and apoptosis pathways in dissociated human prostate cells and evaluate the ability to maintain TMPRSS-ERG+ cells as prostaspheres.

Mentoring (Tasks 1 and 2): Dr. Owen Witte has proven to be the ideal mentor. I attend his group meetings once a month and present data generated in my laboratory for review with his research team. This practice is a valuable source of constructive criticism and idea development. In addition, I have regular, one-on-one mentoring meetings with Dr. Witte to discuss career development, new research ideas, collaborations, and review manuscript/grant proposals every quarter. I will continue this mentoring relationship with Dr. Witte through the term of this grant.

Progress on Specific Aims – Collecting TMPRSS-ERG+ samples: We have continued to expand our collection of human prostate tissue samples. We have collected approximately 60 additional specimens over the past year and generated primary cell cultures. Additionally, we developed a new collaboration with Dr. Jiaoti Huang, a GU pathologist, who assists with tumor isolation from prostate specimens. After the prostate surgical specimens are removed en bloc, an experienced technician from UCLA tissue procurement core laboratory (TPCL) prepares 5 or 6 prostatic sections ranging in thickness from 3-4mm. A sleeve of fresh tissue is obtained from the posterior (peripheral zone) of selected sections. Frozen slides are prepared and stained by H&E staining. Dr. Huang examines the slides and cancerous areas are marked and mapped to the remaining fresh tissue (see appendix figure 1). Tumor nodules were then dissected and isolated from benign tissue. Dissected tissue specimens are processed via mechanical and enzymatic digestion into single cell suspension for in vitro and in vivo culture (method described in appendix, Garraway et al., manuscript *in press*). In addition to enabling tumor nodule isolation, Dr. Huang's lab is developing FISH probes and has in place PCR techniques to detect TMPRSS-ERG fusions. We have employed PCR as a quick way of identifying the translocation in cell lines and primary cultures (see appendix figure 2).

Preserving TMPRSS-ERG+ cells in vitro: As described in the original proposal, we have begun our work to evaluate a variety of culture conditions and the ability to culture TMPRSS-ERG cell in vitro, both as sphere and monolayer cultures. Previous work in this area has indicated that prostate cells cultured in low calcium, serum free media may select for transient amplifying cells(15). We have attempted to culture single cells isolated from dissociated tumor nodules in a variety of media with varying calcium concentrations. In addition to this parameter, we have attempted to block anoikis pathways by adding Rho kinase inhibitors to the media. Using this approach, we have begun to detect TMPRSS-ERG fusion transcript in monolayer cultures (see appendix figure 2). The PCR in figure 2 demonstrates RNA isolated from cells cultured in a variety of conditions with and without Rho kinase inhibition. All of the conditions are performed in duplicate. VCAP is used as a positive control cell line for the TMPRSS-ERG fusion. As seen in the figure, the only sample that contains the TMPRSS-ERG mutation, other than VCAP is sample 8. This sample contained added calcium,

serum, and Rho kinase inhibitor. We are continuing to evaluate whether all TMPRSS-ERG positive tumors can be cultivated under these conditions and if the cells can be expanded and passaged for multiple generations.

Preserving TMPRSS-ERG+ xenografts: In addition to optimizing in vitro conditions for prostate cancer cell growth, we are evaluating conditions that can lead to xenograft formation from primary tumor cells. We have previously developed a technique to regenerate prostate tissue from dissociated cells and prostaspheres (see appendix, Garraway et al., in press and Goldstein et al., submitted). By combining dissociated tumor specimens with urogenital sinus mesenchyme and implanting this cell mix subcutaneously with Matrigel in NOD-SCIDIL2Rγ^{NULL} mice, we have observe the full spectrum of prostate pathology, from benign acini, to cancer foci consistent with Gleason 3 adenocarcinoma (see appendix figure 3). We are currently exploring stromal elements and hormonal/growth factors that can optimize tumor growth. Primary tumor xenografts could be invaluable for future genetic studies in prostate cancer and targeted therapies.

IV - REPORTABLE OUTCOMES:

See appendix for publication and manuscripts submitted/in press related to this work.
Our data has been presented and the AUA Annual meeting in Chicago, April 2009 and at the Prostate Cancer Foundation Annual Retreat in Lake Tahoe, September, 2009.

V - CONCLUSIONS:

Timeline for completion of research tasks documented in the original statement of work is listed below:

Months 0-6:   Initiate cloning of viral vectors; obtain regulatory approval for human and animal research protocols.

Months 7-18:   Collect prostate tissue specimens, attempt to establish new xenografts and monolayer cultures, and begin to evaluate TMPRSS-ERG fusion status in collected tissue specimens via FISH.

Months 19-30: Continue to collect tissue and evaluate for TMPRSS-ERG status. Begin altering growth conditions of dissociated cells that contain the translocation in attempt to preserve cells containing the fusion in vitro. Begin viral-mediated gene transfer of anti-anoikis and anti-apoptosis genes

Months 31-60:   Continue characterization of prostaspheres generated in altered growth environments and upon gene transfer of anti-anoikis/apoptosis genes. Evaluated ability to generate prostaspheres from newly established xenografts.

We have made significant progress in keeping with this timeline, as is evident in the major research accomplishments and are confident that the newfound collaboration with Dr. Huang will continue to propel our efforts forward.

VI - REFERENCES:

1.   Goldstein, A. S., Lawson, D. A., Cheng, D., Sun, W., Garraway, I. P., and Witte, O. N. Trop2 identifies a subpopulation of murine and human prostate basal cells with stem cell characteristics. Proc Natl Acad Sci U S A, *105:* 20882-20887, 2008.
2.   Richardson, G. D., Robson, C. N., Lang, S. H., Neal, D. E., Maitland, N. J., and Collins, A. T. CD133, a novel marker for human prostatic epithelial stem cells. J Cell Sci, *117:* 3539-3545, 2004.
3.   Snoek, R., Rennie, P. S., Kasper, S., Matusik, R. J., and Bruchovsky, N. Induction of cell-free, in vitro transcription by recombinant androgen receptor peptides. J Steroid Biochem Mol Biol, *59:* 243-250, 1996.
4.   Al-Hajj, M. and Clarke, M. F. Self-renewal and solid tumor stem cells. Oncogene, *23:* 7274-7282, 2004.
5.   Singh, S. K., Clarke, I. D., Hide, T., and Dirks, P. B. Cancer stem cells in nervous system tumors. Oncogene, *23:* 7267-7273, 2004.
6.   Dontu, G., Abdallah, W. M., Foley, J. M., Jackson, K. W., Clarke, M. F., Kawamura, M. J., and Wicha, M. S. In vitro propagation and transcriptional profiling of human mammary stem/progenitor cells. Genes Dev, *17:* 1253-1270, 2003.
7.   Bez, A., Corsini, E., Curti, D., Biggiogera, M., Colombo, A., Nicosia, R. F., Pagano, S. F., and Parati, E. A. Neurosphere and neurosphere-forming cells: morphological and ultrastructural characterization. Brain Res, *993:* 18-29, 2003.
8.   Lawson, D. A., Xin, L., Lukacs, R. U., Cheng, D., and Witte, O. N. Isolation and functional characterization of murine prostate stem cells. Proc Natl Acad Sci U S A, *104:* 181-186, 2007.
9.   Xin, L., Lukacs, R. U., Lawson, D. A., Cheng, D., and Witte, O. N. Self renewal and multilineage differentiation in vitro from murine prostate stem cells. Stem Cells, 2007.

10. Tomlins, S. A., Rhodes, D. R., Perner, S., Dhanasekaran, S. M., Mehra, R., Sun, X. W., Varambally, S., Cao, X., Tchinda, J., Kuefer, R., Lee, C., Montie, J. E., Shah, R. B., Pienta, K. J., Rubin, M. A., and Chinnaiyan, A. M. Recurrent fusion of TMPRSS2 and ETS transcription factor genes in prostate cancer. Science, *310:* 644-648, 2005.

11. van Bokhoven, A., Varella-Garcia, M., Korch, C., Hessels, D., and Miller, G. J. Widely used prostate carcinoma cell lines share common origins. Prostate, *47:* 36-51, 2001.

12. Mertz, K. D., Setlur, S. R., Dhanasekaran, S. M., Demichelis, F., Perner, S., Tomlins, S., Tchinda, J., Laxman, B., Vessella, R. L., Beroukhim, R., Lee, C., Chinnaiyan, A. M., and Rubin, M. A. Molecular characterization of TMPRSS2-ERG gene fusion in the NCI-H660 prostate cancer cell line: a new perspective for an old model. Neoplasia, *9:* 200-206, 2007.

13. Collins, A. T. and Maitland, N. J. Prostate cancer stem cells. Eur J Cancer, *42:* 1213-1218, 2006.

14. van Leenders, G. J., Aalders, T. W., Hulsbergen-van de Kaa, C. A., Ruiter, D. J., and Schalken, J. A. Expression of basal cell keratins in human prostate cancer metastases and cell lines. J Pathol, *195:* 563-570, 2001.

15. Litvinov, I. V., Vander Griend, D. J., Xu, Y., Antony, L., Dalrymple, S. L., and Isaacs, J. T. Low-calcium serum-free defined medium selects for growth of normal prostatic epithelial stem cells. Cancer Res, *66:* 8598-8607, 2006.

APPENDIX:

Figure 1

Preservation and Expansion of TMPRSS-ERG+ Cells

Frozen Section

Fresh Prostate tissue

Tumor Mapping

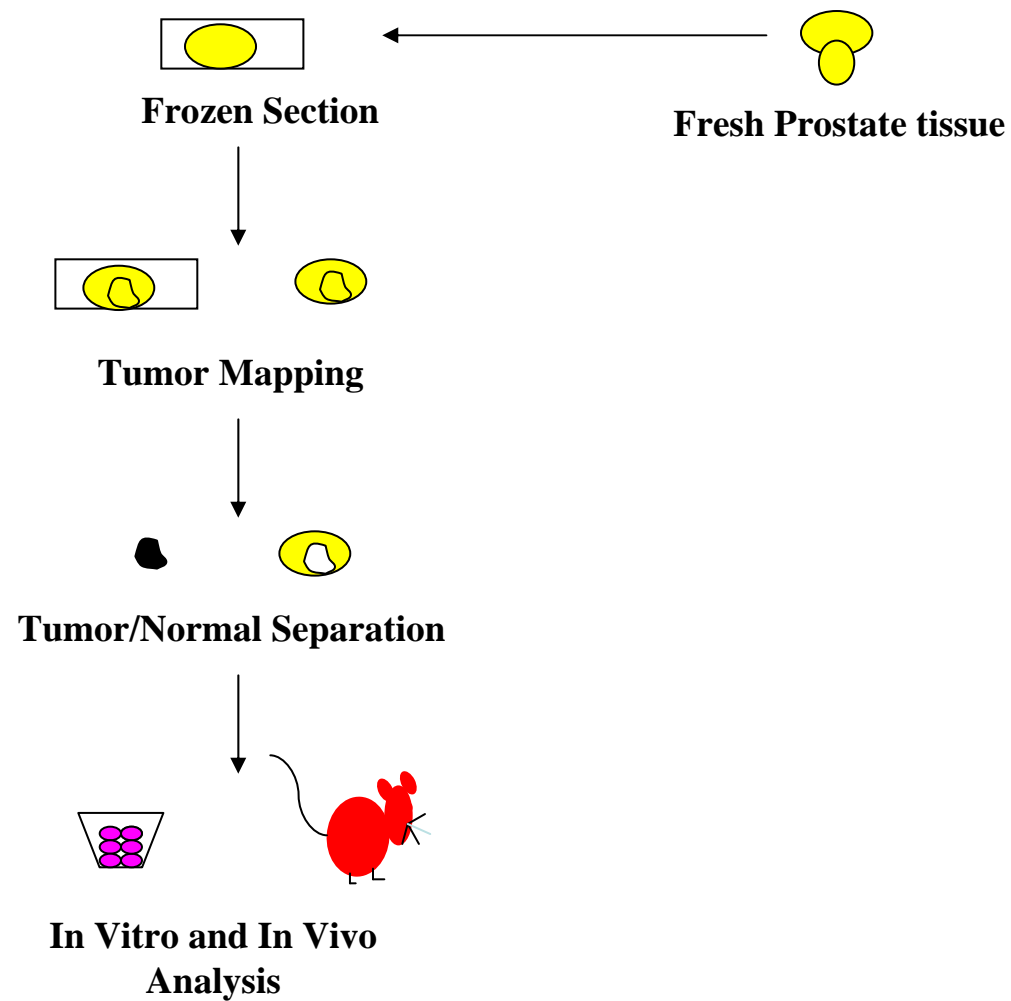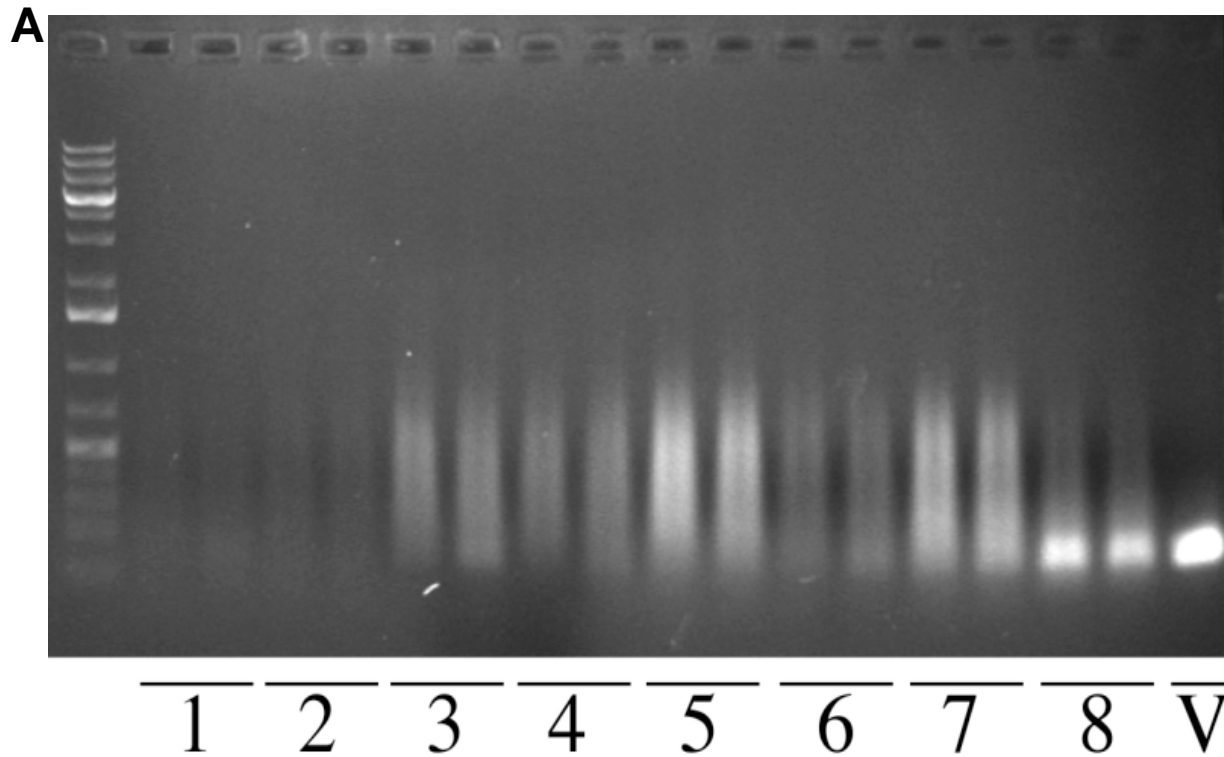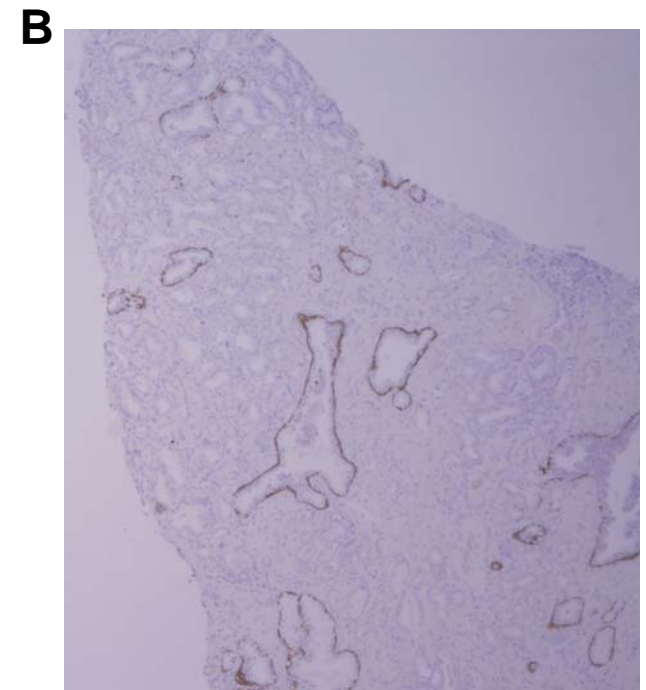**Tumor/Normal Separation**

In Vitro and In Vivo Analysis

Figure 2

Primary prostate cancer cells isolated from tumor nodules and expanded in vitro exhibit TMPRSS-ERG Fusion
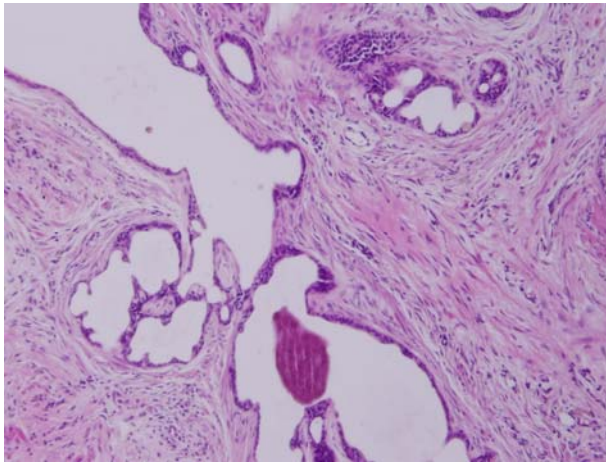

A

1 2 3 4 5 6 7 8 V

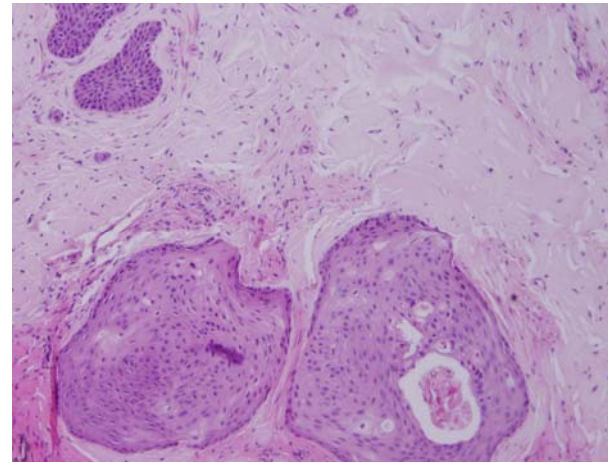V: Vcap cells as a positive control.

B
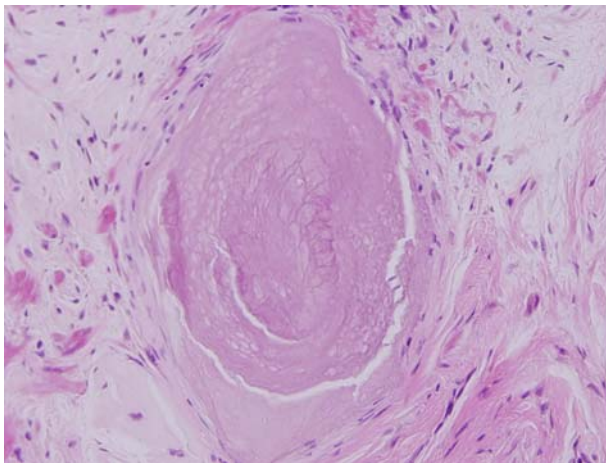
TMPRSS-ERG+ Gleason 4+5 Tumor
stained for CK5

Figure 3

Human Prostate Tissue Regeneration From Dissociated Tumors Demonstrates Pathological Spectrum
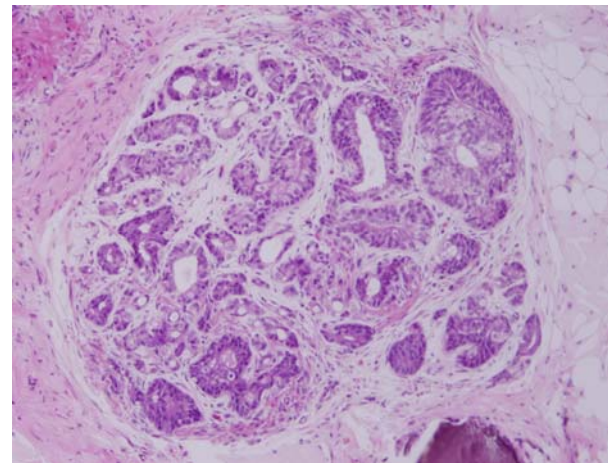
Benign Tubules

Epithelial Cords

Corpora Amylacea

Cancer Foci

The Prostate

Human Prostate Sphere-Forming Cells Represent A Subset of Basal Epithelial Cells Capable of Glandular Regeneration In Vivo

1
2
3
4
5
6
7
8
9
10
11
12
13
14
15
16
17
18
19
20
21
22
23
24
25
26
27
28
29
30
31
32
33
34
35
36
37
38
39
40
41
42
43
44
45
46
47
48
49
50
51
52
53
54
55
56
57
58
59
60

Human Prostate Sphere-Forming Cells Represent A Subset of Basal Epithelial Cells Capable of Glandular Regeneration In Vivo

Isla P. Garraway[1,2]*, Wenyi Sun[1,2], Chau P. Tran[1,2], Sven Perner[3], Bao Zhang[1,2], Andrew S. Goldstein[4], Scott A. Hahm[1], Maahum Haider[1], Christian S. Head[2,5], Robert E. Reiter[1,2], Mark A. Rubin[3], and Owen N. Witte[2, 4, 6]

Running Title: Human Prostate Sphere-Forming Cells

[1]Department of Urology, David Geffen School of Medicine at UCLA

[2]Jonsson Comprehensive Cancer Center

[3]Department of Pathology, Room C-440, Weill Medical Center of Cornell University

[4]Department of Microbiology, Immunology, and Molecular Genetics, UCLA

[5]Division of Head and Neck Surgery, David Geffen School of Medicine at UCLA

[6]Department of Pathology and Clinical Medicine, David Geffen School of Medicine at UCLA

[7]Investigator of the Howard Hughes Medical Institute, Broad ISCBM

*To Whom Correspondence Should Be Addressed: Box 951738 CHS, 10833 LeConte Avenue, LA, CA 90095-1738, 310-206-4890, igarraway@mednet.ucla.edu

Abstract:

Background. Prostate stem/progenitor cells function in glandular development and maintenance. They may be targets for tumor initiation, so characterization of these cells may have therapeutic implications. Cells from dissociated tissues that form spheres in vitro often represent stem/progenitor cells. A subset of human prostate cells that form prostaspheres were evaluated for self-renewal and tissue regeneration capability in the present study.

Methods. Prostaspheres were generated from 59 prostatectomy specimens. Lineage marker expression and TMPRSS-ERG status was determined via immunohistochemistry and fluorescence in situ hybridization (FISH). Subpopulations of prostate epithelial cells were isolated by cell sorting and interrogated for sphere-forming activity. Tissue regeneration potential was assessed by combining sphere-forming cells with rat urogenital sinus mesenchyme (rUGSM) subcutaneously in immunocompromised mice.

Results. Prostate tissue specimens were heterogeneous, containing both benign and malignant (Gleason 3-5) glands. TMPRSS-ERG fusion was found in approximately 70% of cancers examined. Prostaspheres developed from single cells at a variable rate (0.5-4%) and could be serially passaged. A basal phenotype (CD44+CD49f+CK5+p63+CK8-AR-PSA-) was observed among sphere-forming cells. Subpopulations of prostate cells expressing tumor-associated calcium signal transducer 2 (Trop2), CD44, and CD49f preferentially formed spheres. In vivo implantation of sphere-forming cells and rUGSM regenerated tubular structures containing discreet basal and luminal layers. The TMPRSS-ERG fusion was absent in prostaspheres derived from fusion-positive tumor tissue, suggesting a survival/growth advantage of benign prostate epithelial cells.

Conclusion. Human prostate sphere-forming cells self-renew, have tissue regeneration capability, and represent a subpopulation of basal cells.

Introduction:

Adult multipotential stem cells (SCs) are responsible for the development, maintenance, and regeneration of the range of specialized cell types comprising mammalian tissues(1, 2). Self-renewal is a fundamental characteristic of SCs and refers to asymmetric divisions that give rise to genetically identical daughter cells in addition to more differentiated progenitors. Substantial evidence suggests that this process may be deregulated in cancer, as transformed SCs or early progenitors demonstrate uncontrolled self-renewal that results in phenotypically diverse tumors(3-5). Isolation of these cells may allow antigenic/molecular profiling and the delineation of mechanisms that regulate self-renewal and differentiation(5, 6).

Several studies have attempted to identify human prostate SCs (7-12). Richardson et al found that the $\alpha_2\beta_1{}^{hi}$-integrin cells co-expressing CD133 had increased proliferative activity, in vitro and limited tissue regeneration capacity, in vivo(10). The CD133+/ $\alpha_2\beta_1{}^{hi}$ cells represent a small fraction (<1%) of prostate epithelial cells in benign and cancer tissues(8, 10, 12, 13). In a study of non-immortalized and immortalized human prostate cell lines, prostate stem cells were suggested to be CD133+/ABCG2+/ $\alpha_2\beta_1{}^{hi}$/P63-/PSCA-/AR-/PSA- based on the low frequency of these cells in primary prostate epithelial (PrEC) cultures in relation to neuroendocrine and transient amplifying cells(12). Additionally, sorted CD133+ cells yielded cultures containing a mix of CD133+ and CD133- prostate cells, representing the lineage cell types (11, 12).

In order to adequately analyze prostate SCs and hierarchical order of prostate lineage cells derived from human tissue, methods that enable the efficient isolation and expansion of these rare cells is critical. Culture conditions that support proliferation of prostate cells that form spheres may represent a strategy for SC isolation(8, 14-16). Spheres are multicellular globes that develop from cells that survive anchorage-independent conditions in vitro, such as growth in ultra-low attachment (ULA) plates or 3D Matrigel cultures(17). Spheres include SCs and early progenitors in studies of breast, brain, and skin and are frequently used to study the processes of self-renewal and differentiation in these systems(14, 18-20). Lang et al observed human sphere formation from dissociated prostate tissue(21). Spheroid formation and branching morphogenesis

with expression of luminal markers in response to androgen and stromal growth factors was noted when primary human prostate cells were grown in 3D Matrigel cultures(21). Other human studies have suggested that prostasphere formation is a functional validation of prostate SC activity in fractionated cell lines or xenografts(9, 22, 23). In order to further characterize the relationship between stem/progenitor cells and sphere-formation, self-renewal and tissue regeneration properties of prostaspheres should be addressed.

In the present study, a diverse collection of human prostate surgical specimens was accrued and prostaspheres were generated reproducibly and robustly from all prostate tissue types when cells were cultured in low calcium, serum free, defined medium(12). Clonally derived prostaspheres could be dissociated and passaged for multiple generations and induced the formation of ductal/acinar-like structures *in vivo*. Trop2, alpha 6-integrin (CD49f), and CD44 mark cells with enriched sphere-forming capability. The self-renewing and differentiation features of prostaspheres support preservation of SC activity in these cultures. As previously suggested, low calcium, serum free culture conditions that support human prostate stem/progenitor growth appears to select exclusively for normal cells, since the *TMPRSS-ERG* fusion was never observed in the prostaspheres derived from fusion positive tissue specimens(11, 12, 24).

Materials and Methods:

Tissue acquisition, isolation and culture of prostate epithelial cells:
Human prostate tissue was obtained from 59 patients (ages 41-76), undergoing prostate surgery (radical prostatectomy or cystoprostatectomy). All subjects were consented for tissue collection in accordance with an approved protocol through the Office for the Protection of Research Subjects at UCLA. For a list of patient characteristics, see supplemental Table 1. Adjacent tissue specimens were fixed in formalin and paraffin-embedded to determine the presence of benign or malignant glands. The remainder of the tissue specimens were mechanically and enzymatically digested as previously described(25). Dissociated prostate cell suspensions were sequentially filtered through 100-micron and 40-micron filters, and then passed through a 23-gauge needle. Cells

were counted with a hemocytometer and resuspended in PREGM (Clonetics) supplemented with FGF2 (Invitrogen), EGF (Sigma), B27 (Invitrogen), and heparin (Sigma). The cells were then cultured (as described below), or subjected to cell separation using MACS beads columns (Miltenyi Biotec LTD, Surrey, UK) or a cell sorter, as described below.

Antigenic cell separation:

Cells were mixed with MACS microbeads linked to a cocktail of lineage antibodies (Lineage Depletion Kit, Miltenyi Biotec Ltd, Surrey, UK). After selection through the magnetic column, lineage negative cells were incubated with Trop-2 (R&D Systems), anti-CD44 (Abcam), anti-CD49f (Biolegend), or anti-CD133 (Miltenyi) antibodies, followed by incubation with MACS goat anti-mouse IgG microbeads (Miltenyi) and application to a MACS column. Alternatively, Lin- cells stained with fluorescent-linked primary antibody were subjected to sorting. Sorted cells were counted and plated in 3D Matrigel cultures.

In vitro prostasphere culture:

Epithelial cells were counted and re-suspended in 50:50 matrigel:PREGM a concentration of $1x10^3$-$6x10^4$ cells/80microliters. This matrigel/cellular suspension was plated at the edge of the well on 12-well plates and allowed to set by incubation at 37^0C for 30 minutes. One milliliter of defined media was then added to each well and plates were replaced in 37^0C incubator. For dissociation and passage of prostaspheres, 1-hour incubation in 1mg/ml Dispase (Invitrogen) was performed. Spheres were collected, washed in RPMI, and trypsinized (TripLE 100microliters/12-well plate). Cells were washed, counted, and replated as described above.

Lentiviral infection of prostate epithelial cells:

Prostate epithelial cells were cultured in PREGM for 48-72 hours. Viral supernatant containing lentivirus (CCR-dsRed, a gift from the laboratory of Dr. Irvin Chen at UCLA) and polybrene was added for 3 hours at 37^0C. Red fluorescence was detected 48-72

hours post-infection. Monolayer cells were detached with TripLE and plated in Matrigel for sphere formation.

Immunohistochemistry of tissue/prostasphere sections:

Prostate tissue was paraffin embedded as previously described(26). For paraffin embedding of prostaspheres, matrigel cultures were subjected to Dispase (1mg/ml, Invitrogen) and whole prostaspheres were collected and fixed in 10% buffered formalin at 4^0C for twelve hours. After fixation, prostaspheres were washed in PBS and 50% ethanol, pelleted by centrifugation, and resuspended in 10-20microliters of Histogel (Richard-Allen Scientific). Four-micron thick sections of frozen or paraffin embedded tissue were deparaffinized with xylene and rehydrated through a descending series of ethanol washes as described. Antigen retrieval and standard immunoperoxidase procedures were used in combination with primary antibodies. For Immunofluorescence assays, permeablization of tissue was performed using cold methanol:acetone, followed by staining with antibodies.

Fluorescence-activated cell sorting and analysis:

Prostate cells were suspended in PBS/10% FCS and stained with antibody for 30 minutes at 4^0C. Fluorescence-activated cell sorting and analysis are performed on a BD Special Order FACSAria II system and Diva v6.1.1. Live single cells are gated based on scatter properties and analyzed for their surface marker expression. Cells are sorted and collected at 40C using 100um nozzle and 23psi.

Subcutaneous Injections in Immunocompromised mice:

Male SCID mice age 8-24 weeks was subjected to subcutaneous injections of prostaspheres +/- 2 x 10^5 rat urogenital sinus mesenchyme (rUGSM) suspended in 100 microliters 50:50 matrigel:PREGM. Subcutaneous implantation of time-release testosterone pellets was performed. Subcutaneous nodules at the site of injection were removed and frozen/paraffin-embedded sections were generated for immunohistochemical analysis. Rat UGSM was prepared as previously described (27).

Fresh UGSM cells were cultured in DMEM+10%FBS and passaged twice prior to use in tissue regeneration assays.

Fluorescence Activated In Situ Hybridization:

Paraffin-embedded human prostate tumor specimens were subjected to FISH as previously described(28). Briefly, the break-apart assay is utilized with probes that recognize the centromeric and telomeric portions of the ERG gene. If there is a break in the gene, distinct red and green signals are detected. If the gene is intact, the red and green probes remain adjacent and sometimes overlap, resulting in a yellow signal (See Figure 4).

Results:

A small fraction human prostate cells obtained from a diverse collection of human prostate tumor specimens form prostaspheres

To investigate whether sphere-forming cells may be derived from all types of human prostate tissue, specimens were obtained from 59 patients undergoing radical prostatectomy or cystoprostatectomy. Pathological examination of collected specimens confirmed inclusion of either benign (normal and BPH) or a mixture of benign and malignant glands with Gleason grades ranging from 3-5 (Supplemental Table 1). Fresh tissues were mechanically and enzymatically dissociated and single cells were seeded in ULA plates or Matrigel at densities ranging from 10^2 to 10^5 cells/well (Figure 1, Supplemental Figure 1). Prostaspheres formed from 21/24 specimens cultured in ULA plates and 35/35 specimens cultured in Matrigel within 3 days of plating, with continued growth over 2 weeks to diameters of 100-400 microns (Figure 1). There were only three patient specimens that failed to for prostaspheres, which may be attributed to variations in tissue processing as conditions were worked out. We observed that Matrigel cultures facilitated enumeration of prostaspheres by preventing the aggregation of cells that occurs in floating culture (14, 29). Sphere architecture and marker expression was similar in both growth conditions (Supplemental Figure 1).

Although significant variability in the number of prostaspheres that developed from individual patient specimens was observed, consistent variation in the number or appearance of prostaspheres according to specific clinical or pathological parameters was not apparent (Figure 1A-B). Further prospective analysis with dissection/isolation of tumor nodules may allow more definitive conclusions on the relationship of sphere-formation and Gleason grade. Tallies of prostaspheres were obtained from a sample of 10 individual patients with varying pathologies (benign to malignant) after replicate plating in 6-well culture dishes. The average number of prostaspheres obtained with similar seeding densities per patient was plotted (Figure 1B). The frequency of sphere-forming cells derived from all 59 patients was found to range from approximately 0.5%-4% (data not shown).

Human prostaspheres are clonally derived and self-renew

To confirm the clonal origin of prostaspheres, 10^5 freshly isolated prostate epithelial cells were grown as a monolayer for 48 hours and then labeled with red fluorescent protein via lentiviral-mediated gene transfer of the dsRed gene. Approximately 90% of prostate cells appeared to be expressing dsRed within seventy-two hours after exposure to virus (data not shown). Infected (red) prostate epithelial cells were detached and mixed with wild-type (colorless) cells at a ratio of 1:5. The mixed cell populations were plated in Matrigel in triplicate. Approximately 7 days following plating, robust prostasphere formation was observed and only monochromatic (all red or all colorless) prostaspheres were identified, consistent with the concept of clonality (Figure 1C). Microscopic examination of frozen sections of DSRED and clear prostaspheres demonstrated that all cells within a single sphere were monochromatic (Figure 1C-E).

All of the prostasphere specimens cultured in Matrigel could be passaged for multiple generations. Repetitive passaging was specifically assessed in 4 individual prostasphere cultures and more than 20 generations were obtained without any sign of growth decline after dissociation and passage (data not shown). DsRed-infected prostaspheres could also be dissociated, mixed, and passaged repeatedly (>3 generations) with formation of new monochromatic prostaspheres. Single red fluorescent

prostaspheres were isolated by serial dilution in 96-well plates, followed by dissociation and incubation of single cells in Matrigel. Secondary red prostaspheres were noted to develop, supporting the self-renewal potential of individual prostaspheres (Figure 1C-F).

Prostate cells obtained from dissociated prostaspheres also remained viable after freeze/thaw, with formation of new spheres in Matrigel that could be serially passaged. Dissociated prostaspheres (passage 2-10) were cryopreserved for 1 month followed by thaw and seeding in Matrigel. New prostaspheres developed 7-10 days after plating that could be passaged >3 generations (data not shown). Taken together, these findings highlight the versatility of prostaspheres, in that they can be genetically manipulated, expanded continuously in vitro, and cryopreserved.

Prostaspheres express predominately basal markers

The prostate epithelium is composed of basal cells, including stem cells and transient amplifying cells, terminally differentiated luminal cells, and neuroendocrine cells(30). Prostate epithelial cells can be differentiated based on expression of a variety of markers(31). The majority of basal cells express the high molecular weight cytokeratins (CK5 and CK14), p63, CD44, alpha integrin, and do not express significant low molecular weight cytokeratins (CK8/18), AR or PSA(12, 25). Luminal cells, in contrast, do not express p63, but exhibit relatively high levels of AR, PSA, CK8/18(31). Transient amplifying (intermediate) cells express basal marker, CK5 and often co-express the luminal marker, CK8 and prostate stem cell antigen (PSCA)(25). Neuroendocrine cells are express neuropeptides, including chromogranin A and synaptophysin(31).

In order to determine the expression profile of prostate epithelial cells within prostaspheres, immunostaining was performed using antibodies against several basal and luminal markers (Figure 2A). The basal markers CK5, alpha 6 integrin (CD49f), CD44, and p63 were strongly expressed by the majority of sphere-forming cells. Greater than 95% of the sphere-forming cells/20X objective high-powered field (hpf) appeared to express CK5 and p63. Between 50-80% of cells/hpf expressed CD44 and CD49f. Luminal markers, including AR (androgen receptor) and PSA (prostate-specific antigen) were not observed in prostaspheres (data not shown). CK8 expression was noted in approximately 1% of sphere-forming cells/hpf. Co-expression with CK5 was seen in

these cells (Figure 2A). We did not observe cells expressing the neuroendocrine markers, synaptophysin or Chromogranin A (data not shown).

In addition to prostatic markers, the spheres were assessed for cell proliferation and apoptosis via Ki-67 and TUNEL staining (Supplemental Figure 2). Approximately 2% of the sphere cells/hpf were observed to have Ki-67 activity, with the outermost layer of the sphere demonstrating the most activity. TUNEL staining was not clearly detected in prostaspheres (Supplemental Figure 2).

Antigenic profile of human prostasphere-forming cells

To determine the surface markers that identify cells capable of prostasphere formation, we fractionated subpopulations of prostate cells via microbeads or automatic cell sorter separation (Figure 2B-D). Cell fractionation resulted in a variable decrease (2-10 fold) in the overall number of prostaspheres formed following manipulation secondary to decreased cell viability following these manipulations (data not shown). However, comparison of fractionated cell populations within individual specimens allowed relative sphere-forming activity to be assessed.

In order to eliminate the possibility that cells of the hematopoeitic lineage retained in the prostate tissue contributed to the sphere-forming population, we performed depletions with blood lineage antibodies. FACS analysis with representative lineage antibodies CD31 and CD45 confirmed removal of hematopoeitic/endothelial cells (Supplemental 3B). Lin- and Lin+ cells were plated in Matrigel cultures in several replicates of $1x10^4$cells/well to assess sphere-forming activity. Prostaspheres formed exclusively in the Lin- cell fraction (Figure 2B).

Previous investigations of human and murine prostate SCs have suggested that CD44 may be an important marker(10). In order to investigate whether CD44+ prostate epithelial cells were enriched for sphere-forming capability, we used microbeads or automatic cell sorting to isolate cells expressing this antigen. FACS analysis confirmed enrichment of CD44+ cells (Supplemental Figure 3B). Plating of CD44+ cells in Matrigel demonstrated enriched sphere-forming capability (>2.5-fold) with 1/15 Lin-CD44+ cells forming spheres (Figure 2B). Although the presence of CD44 greatly enriched for sphere-forming capability, some spheres were noted in the Lin-CD44-

fraction. This likely represents incomplete separation of CD44+ and CD44- cells, but the possible that a fraction of Lin-CD44- cells have sphere-forming capability cannot be excluded.

We used a similar approach to examine whether CD49f or the putative human prostate stem cell marker, CD133, marked the sphere-forming population. FACS analysis demonstrated CD49f+ (8-20%) and CD133+ cells (2-7%) after lineage depletion (data not shown). Fractionated prostate cells were evaluated by FACS prior to seeding in Matrigel (Supplemental Figure 3B). A marked increase in sphere formation was observed with Lin-CD49f+ cells compared to Lin-CD49f- cells (Figure 2B). On the other hand, multiple attempts to separate CD133+ and CD133- cells resulted in highly variable results in sphere-forming capability. For most of the patient samples, more spheres appeared to form in the CD133- fraction, however, a smaller number of spheres consistently formed within the CD133+ fraction as well (Figure 2B). Our difficulties in obtaining consistent results with CD133 cell separation could be due to the fact that the CD133+ cells are so rare, usually composing 0.25-2% of unfractionated prostate cells. This made isolation and plating in sphere cultures difficult. We typically isolated $<2 \times 10^3$ CD133+ cells via this approach. Alternatively, CD133 as a solitary marker may subdivide, but not distinguish the sphere-forming population.

Our previous studies have demonstrated that human prostate sphere-forming cells are similar to murine prostate sphere-forming cells in regard to antigenic profile. The epithelial marker, Trop-2 in combination with the high expression of the integrin, CD49f (a marker of human basal cells), enables sphere-forming cells to be isolated. Trop-2 expression appears confined to epithelial cells in the human prostate and may be used in combination with other markers to evaluate subpopulations of prostate epithelial cells for sphere-forming capability. We performed cell sorting based on Trop2/CD49f and Trop2/CD44 expression and found that the double positive fractions (Trop2+CD49fHI and Trop2+CD44+) demonstrate the highest sphere-forming capability in multiple patients (Figure 2C-D).

Prostaspheres do not contain the *TMPRSS-ERG* gene rearrangement

Since the human prostaspheres were generated from primary tumors that contain a heterogeneous mix of benign and malignant glands, evaluation to distinguish benign and cancerous spheres, was warranted. However, qualitative and quantitative differences were not observed among prostaspheres derived from different pathological specimens (Figure 1). With the discovery of prevalent gene rearrangements involving ETS family members in prostate cancer, we predicted that cytogenetic tools may enable identification of cancerous prostaspheres(28). Gene fusions involving *ERG*, *ETV1*, and *ETV4* involve a variety of 5' partners that direct aberrant expression of these transcription factors and may initiate a cascade of events leading to tumorigenesis(28). The most common rearrangement involves juxtaposition of the androgen-regulated *TMPRSS2* gene with *ERG*. *TMPRSS-ERG* gene fusions have been detected in primary prostate tumor specimens, metastases, and xenografts by fluorescence in situ hybridization (FISH)(28). Analysis of prostate tumor surgical cohorts have found 36-78% of prostate cancers possess the *TMPRSS-ERG* fusion(28). The presence of this fusion in individual prostaspheres may suggest that cancer stem/early progenitor cells are expanded in our cultures.

To test the feasibility of this approach, FISH analysis was performed on select prostate tissue specimens and coordinating prostaspheres (Figure 3). The *TMPRSS-ERG* fusion was found in approximately 7/10 (70%) cancer cases tested (Figure 3A). The fusion, however, was consistently absent in prostasphere cultures derived from *TMPRSS-ERG+* tissues, even when the specimens obtained contained >80% tumor (Figure 3B-E). Analysis of monolayer cultures concomitantly derived from prostate tumor specimens also failed to demonstrate the presence of the gene fusion, indicating that both spheroid and adherent cultures select for fusion-negative, genetically normal cells (data not shown).

Sphere-mediated prostate tissue regeneration:

To evaluate whether human prostaspheres can form ductal/acini structures in vivo, whole prostaspheres from eight patients were injected subcutaneously into NOD-SCID/IL2rγNull mice with or without $2x10^5$ rUGSM cells. The number of sphere forming cells injected ranged from $5x10^4$ to $1x10^6$. All experiments were performed in duplicate. In the mice injected with whole prostaspheres combined with Matrigel, 10/16

grafts were obtained 6-12 weeks post injection (Figure 4A). The grafts ranged in weight between approximately 25 mg and 250 mg. Control mice injected with rat UGSM without prostaspheres, were included for comparison (Figure 4A). Grafts were fixed in formalin and embedded in paraffin to prepare tissue sections. H&E staining revealed the prostaspheres induced formation of acinar-like structures. No acini were observed in the rUGSM only grafts. In the absence of rUGSM, prostaspheres induced the development of rudimentary appearing acini/epithelial cords with multiple layers of epithelial cells and rare lumen formation (Figure 4A). On the other hand, when human prostaspheres were combined with rat rUGSM and Matrigel, acini contained well-defined lumens with secretions (Figure 4A). IHC analysis showed that these acinar structures were reminiscent of normal adult human adult prostate glands with CK8 and AR positive luminal cells as well as CK5 and p63 positive basal cells (Figure 4B). Human prostate-specific markers, prostate stem cell antigen (PSCA), prostate membrane antigen (PSMA), and prostate specific antigen (PSA) were also observed (Figure 4B). Immunostaining for the neuroendocrine markers synaptophysin and chromogranin A did not demonstrate neuroendocrine cells (data not shown). Although prostaspheres regenerated xenografts resembling normal human prostate, the efficiency of glandular structure formation was relatively low with 1-12 tubules ranging per 20X/hpf. Our results indicate that prostaspheres are capable of glandular regeneration with basal and luminal compartments comparable to normal human prostate tissue.

Discussion:

Sphere-formation in anchorage-independent conditions is a characteristic of SCs initially described in neural and mammary systems(16, 18). Studies of murine prostate have demonstrated that a small fraction of prostate epithelial cells expressing Sca-1 and alpha-6 integrin (CD49f), and Trop2 formed spheres in 3D-Matrigel cultures that possessed self-renewal and differentiation characteristics(14, 17, 21, 32). Additionally, only the sphere-forming fraction of murine prostate epithelial cells can induce gland formation via in vivo tissue regeneration(17, 33). In human studies, in vitro prostate spheroid formation with branching morphogenesis has been observed, but self-renewal, tissue regeneration capability, and antigenic profiling to delineate the sphere-forming

population was not addressed(32, 34). Here, we show that 0.5%-4% of epithelial cells obtained from a wide variety of dissociated human prostate specimens form prostaspheres that possess features of self-renewal, as demonstrated by serial passage. Human prostaspheres can also be dissociated and cryopreserved with the retention of sphere-forming ability following thaw (data not shown). These practical traits of human prostaspheres enable viable repositories of prostate stem/progenitor cells to be generated that could facilitate high throughput studies of large collections of patient specimens in the future.

In prior human prostate stem cell studies, epithelial cells expressing $\alpha_2\beta_1^{hi}$ integrin, CD44, and CD133 have displayed stem-like qualities of increased proliferative potential in vitro and regeneration of acinar-like structures in vivo(7, 10, 13). Consistent with previous reports characterizing prostate SCs, the putative SC markers, CD44 and α_6 integrin (CD49f) appeared to greatly enhance for the sphere-forming population in this study, in addition to the epithelial marker, Trop2. The CD133+ population was technically difficult to evaluate, given the small fraction of these cells present in human prostate tissue specimens. Furthermore, recent studies suggest that CD133 antibody binding may inhibit survival of these cells in vitro(11). It was observed that expression of CD133 did not segregate basal epithelial cells based on sphere-forming capability, since both CD133+ and CD133- fractions formed spheres. In contrast to CD44 and CD49f, immunostaining and FACS of prostaspheres failed to detect CD133, indicating that this marker is not preserved in prostasphere cultures (data not shown). The significance of CD133 expression should be evaluated in future studies examining characteristics of prostaspheres capable of tubule formation in vivo (see below).

The marker profile of sphere-forming cells with abundant expression of CK5 and p63 suggest that normal basal cells were selected in our prostasphere cultures. Basal markers are frequently lost in cancer and malignant glands display a luminal phenotype that includes abundant CK8/18 and AR expression, with loss of CK5 and p63(35). Until the discovery of ETS translocations, antigenic or genetic marker that clearly delineated normal and cancerous prostate cells were not available. With ETS family fusions now detectable via FISH, genetic events associated with malignancy can be evaluated in prostaspheres(28, 36). Consistent with the benign basal marker profile of prostaspheres

and regenerated tubules, the *TMPRSS-ERG* fusion was not identified in sphere-forming cells from fusion+ tissue specimens. Although some of the collected tissue specimens contained large tumor volumes (>80% tumor glands), all of the prostaspheres demonstrated a predominance of benign basal cells. Although it is possible that prostate cancer stem/progenitor cells do not contain gene rearrangements, a more likely scenario is that the culture conditions that support human prostate SC isolation and expansion inhibit cancer cell outgrowth. This observation is consistent with previous studies suggesting that cancer cells do not proliferate in the defined medium typically used to expand prostate epithelial cells(12, 24). Dissection of tumor nodules and outgrowth in more permissive media conditions may enable selection of prostate CSCs and will have to be addressed in future studies (24).

The acinar structures observed in vivo also appeared to resemble normal human prostate tissue, with preservation of discreet basal and luminal layers. In vivo tissue regeneration occurred at low efficiency with approximately $1x10^6$ sphere forming cells yielding scant tubules in regenerated grafts. One possibility for the limited differentiation potential of prostaspheres is that a significant proportion of develop from progenitor cells, not bona fide SCs, and are not capable of tubule formation/maturation. To distinguish between human prostate SCs and progenitors, it will be necessary to further subdivide sphere-forming cells and evaluate tissue regeneration capacity of fractionated sphere-forming cells. It is possible that bona fide SCs will have the exclusive ability to recapitulate prostate glands in vivo, while progenitors will demonstrate restricted differentiation.

Conclusions:

Prostate sphere-forming cells include stem/progenitor cells that are capable of self-renewal and tissue regeneration. Sphere forming cells exhibit a basal profile that resembles benign prostate epithelial cells and induce the formation of ductal/acinar structures *in vivo*.

Acknowledgements:

Figure Legends:

Figure 1: Formation of Prostaspheres from Dissociated Human Prostate Tissue. Prostate tissue obtained from patients undergoing cancer surgery was mechanically and enzymatically digested. Single cells were and plated in Matrigel seeded at a density $2x10^4$/well in 6-well culture dishes. Adjacent tissue samples were paraffin-embedded and stained with H&E for histological evaluation. Human prostaspheres developed robustly from all prostate specimens (A), including benign prostate tissue, low-grade (Gleason 3+3) adenocarcinoma, and high-grade (Gleason 4+5) adenocarcinoma. Prostaspheres derived from these tissues formed prostaspheres in Matrigel (A, lower panel). B. Prostaspheres were plated in triplicate in 6-well plates at a seeding density of 1x10e4 cells/well. After approximately 14 days, prostaspheres were counted and the average number of spheres from 7 individual patients with pathological diagnosis of benign prostate, low- grade, and high-grade adenocarcinoma is depicted in the graph. Freshly dissociated prostate cells were grown as a monolayer for 48 hours followed by incubation with lentivirus carrying the gene for red fluorescent protein (RFP). Red cells were mixed with uninfected (colorless) cells at a ratio of 1:5 and plated in Matrigel culture ($1x10^4$ cells/well). Only monochromatic spheres were observed in (C) as seen in light and fluorescent views. Monochromatic spheres were isolated and plated by serial dilution into ULA 96-well plates so that 1-sphere/well was obtained. Single spheres were subjected to digest with TrypLE and single cells were then re-incubated in PREGM media (D). New monochromatic spheres were noted to form from single cells after 2-weeks of incubation (E). Frozen sections of RFP/clear spheres demonstrate that all cells within the sphere are red or clear and confirm clonogenicity (F).

Figure 2: Human prostaspheres exhibit a predominately basal expression profile. Paraffin-embedded human prostaspheres were stained for prostate epithelial markers (A). H&E staining, CD44 (green), CK5 (green), CK8 (red), and p63 (blue) are shown individually as well as co-staining. B. Fractionation of dissociated prostate cells subjected via enrichment/depletion of lineage, CD44, CD49f, or CD133 antigens demonstrate sphere-forming capability of these cell populations. At least 3 different

patient samples were tested per antigen. Lineage, CD44, and CD49f isolates were plated at a rate of $1x10^4$ cells per well. CD133 isolates were plated at $1 x10^3$ cells/well. C, D. Percentage of spheres formed from prostate epithelial cells sorted based on Trop2/CD44 and Trop2/CD49f expression.

Figure 3: Patients undergoing radical prostatectomy for prostate cancer were consented for tissue donation according to an approved protocol through the Office for the Protection of Research Subjects at UCLA. Patient information including age, pre-operative prostate specific antigen (PSA), tumor location on final pathology (R, Right, L, Left, A, Anterior, P, Posterior, Ap, Apex, B, Base), and pathological stage (T2, tumor confined within the prostatic capsule, T3, tumor extends beyond the prostate capsule) is presented in the panel A. Tissue specimens from these patients were mechanically and enzymatically dissociated and cultured in 50:50 Matrigel:PREGM (supplemented with EGF, FGF, and B27) to allow prostasphere formation. Paraffin-embedded tumor specimens and prostaspheres were subjected to FISH for *TMPRSS-ERG* gene rearrangement. Human prostate cancer FISH is shown in panels B (40X) and C (100X) in a case that displays the ERG break-apart genetic variation. In contrast, FISH of the prostaspheres shown in panels D and E show an intact *ERG* gene with overlap of the probes. None of the prostaspheres derived from patients with *TMPRSS-ERG* fusion in their cancer specimens displayed a similar genetic abnormality.

Figure 4: Prostaspheres form acinar structures in immunocompromised mice. Whole prostaspheres were isolated, mixed with Matrigel and injected subcutaneously into mice either with or without rUGSM. Glandular structures could be palpated 6-12 weeks post-injection. Glandular-like structures recovered 8 weeks after subcutaneous implantation of whole prostaspheres (containing from $5x10^4$ to $1x10^6$ cells) suspended in Matrigel. A. H&E staining of graft containing $2x10^5$ rat UGSM only, graft containing regenerated prostate tissue induced by prostaspheres without UGSM, showing tightly packed acinar structures separated by mouse infiltrating stroma, and grafts of regenerated prostate tissue formed by combining whole prostaspheres with $2x10^5$ rat UGSM. B. IHC analysis of

1
2
3
4
5
6
7
8
9
10
11
12
13
14
15
16
17
18
19
20
21
22
23
24
25
26
27
28
29
30
31
32
33
34
35
36
37
38
39
40
41
42
43
44
45
46
47
48
49
50
51
52
53
54
55
56
57
58
59
60

the expression of CK5, p63, PSCA, AR, CK8, and PSA in normal human prostate tissue sections and acini derived induced by prostaspheres (regenerated graft).

REFERENCES

1. Majka, M., Kucia, M., and Ratajczak, M. Z. Stem cell biology - a never ending quest for understanding. Acta Biochim Pol, *52:* 353-358, 2005.

2. Moore, K. A. and Lemischka, I. R. Stem cells and their niches. Science, *311:* 1880-1885, 2006.

3. Polyak, K. and Hahn, W. C. Roots and stems: stem cells in cancer. Nat Med, *12:* 296-300, 2006.

4. Cozzio, A., Passegue, E., Ayton, P. M., Karsunky, H., Cleary, M. L., and Weissman, I. L. Similar MLL-associated leukemias arising from self-renewing stem cells and short-lived myeloid progenitors. Genes Dev, Vol. 17, pp. 3029-3035. 2003.

5. Al-Hajj, M. and Clarke, M. F. Self-renewal and solid tumor stem cells. Oncogene, *23:* 7274-7282, 2004.

6. Jordan, C. T., Guzman, M. L., and Noble, M. Cancer stem cells. N Engl J Med, *355:* 1253-1261, 2006.

7. Collins, A. T., Habib, F. K., Maitland, N. J., and Neal, D. E. Identification and isolation of human prostate epithelial stem cells based on alpha(2)beta(1)-integrin expression. J Cell Sci, *114:* 3865-3872, 2001.

8. Brown, M. D., Gilmore, P. E., Hart, C. A., Samuel, J. D., Ramani, V. A., George, N. J., and Clarke, N. W. Characterization of benign and malignant prostate epithelial Hoechst 33342 side populations. Prostate, *67:* 1384-1396, 2007.

9. Gu, G., Yuan, J., Wills, M., and Kasper, S. Prostate cancer cells with stem cell characteristics reconstitute the original human tumor in vivo. Cancer Res, *67:* 4807-4815, 2007.

10. Richardson, G. D., Robson, C. N., Lang, S. H., Neal, D. E., Maitland, N. J., and Collins, A. T. CD133, a novel marker for human prostatic epithelial stem cells. J Cell Sci, *117:* 3539-3545, 2004.

11. Vander Griend, D. J., Karthaus, W. L., Dalrymple, S., Meeker, A., DeMarzo, A. M., and Isaacs, J. T. The role of CD133 in normal human prostate stem cells and malignant cancer-initiating cells. Cancer Res, *68:* 9703-9711, 2008.

12. Litvinov, I. V., Vander Griend, D. J., Xu, Y., Antony, L., Dalrymple, S. L., and Isaacs, J. T. Low-calcium serum-free defined medium selects for growth of normal prostatic epithelial stem cells. Cancer Res, *66:* 8598-8607, 2006.

13. Collins, A. T., Berry, P. A., Hyde, C., Stower, M. J., and Maitland, N. J. Prospective identification of tumorigenic prostate cancer stem cells. Cancer Res, *65:* 10946-10951, 2005.

14. Lawson, D. A., Xin, L., Lukacs, R. U., Cheng, D., and Witte, O. N. Isolation and functional characterization of murine prostate stem cells. Proc Natl Acad Sci U S A, *104:* 181-186, 2007.

15. Wang, T. Y., Sen, A., Behie, L. A., and Kallos, M. S. Dynamic behavior of cells within neurospheres in expanding populations of neural precursors. Brain Res, *1107:* 82-96, 2006.

16. Ishibashi, S., Sakaguchi, M., Kuroiwa, T., Yamasaki, M., Kanemura, Y., Shizuko, I., Shimazaki, T., Onodera, M., Okano, H., and Mizusawa, H. Human neural

stem/progenitor cells, expanded in long-term neurosphere culture, promote functional recovery after focal ischemia in Mongolian gerbils. J Neurosci Res, *78:* 215-223, 2004.

17. Goldstein, A. S., Lawson, D. A., Cheng, D., Sun, W., Garraway, I. P., and Witte, O. N. Trop2 identifies a subpopulation of murine and human prostate basal cells with stem cell characteristics. Proc Natl Acad Sci U S A, *105:* 20882-20887, 2008.

18. Dontu, G., Abdallah, W. M., Foley, J. M., Jackson, K. W., Clarke, M. F., Kawamura, M. J., and Wicha, M. S. In vitro propagation and transcriptional profiling of human mammary stem/progenitor cells. Genes Dev, *17:* 1253-1270, 2003.

19. Bez, A., Corsini, E., Curti, D., Biggiogera, M., Colombo, A., Nicosia, R. F., Pagano, S. F., and Parati, E. A. Neurosphere and neurosphere-forming cells: morphological and ultrastructural characterization. Brain Res, *993:* 18-29, 2003.

20. Blatchford, D. R., Quarrie, L. H., Tonner, E., McCarthy, C., Flint, D. J., and Wilde, C. J. Influence of microenvironment on mammary epithelial cell survival in primary culture. J Cell Physiol, *181:* 304-311, 1999.

21. Lang, S. H., Sharrard, R. M., Stark, M., Villette, J. M., and Maitland, N. J. Prostate epithelial cell lines form spheroids with evidence of glandular differentiation in three-dimensional Matrigel cultures. Br J Cancer, *85:* 590-599, 2001.

22. Snoek, R., Rennie, P. S., Kasper, S., Matusik, R. J., and Bruchovsky, N. Induction of cell-free, in vitro transcription by recombinant androgen receptor peptides. J Steroid Biochem Mol Biol, *59:* 243-250, 1996.

23. Tang, D. G., Patrawala, L., Calhoun, T., Bhatia, B., Choy, G., Schneider-Broussard, R., and Jeter, C. Prostate cancer stem/progenitor cells: identification, characterization, and implications. Mol Carcinog, *46:* 1-14, 2007.

24. Dalrymple, S., Antony, L., Xu, Y., Uzgare, A. R., Arnold, J. T., Savaugeot, J., Sokoll, L. J., De Marzo, A. M., and Isaacs, J. T. Role of notch-1 and E-cadherin in the differential response to calcium in culturing normal versus malignant prostate cells. Cancer Res, *65:* 9269-9279, 2005.

25. Tran, C. P., Lin, C., Yamashiro, J., and Reiter, R. E. Prostate stem cell antigen is a marker of late intermediate prostate epithelial cells. Mol Cancer Res, *1:* 113-121, 2002.

26. Garraway, I. P., Seligson, D., Said, J., Horvath, S., and Reiter, R. E. Trefoil factor 3 is overexpressed in human prostate cancer. Prostate, *61:* 209-214, 2004.

27. Hayward, S. W., Haughney, P. C., Rosen, M. A., Greulich, K. M., Weier, H. U., Dahiya, R., and Cunha, G. R. Interactions between adult human prostatic epithelium and rat urogenital sinus mesenchyme in a tissue recombination model. Differentiation, *63:* 131-140, 1998.

28. Tomlins, S. A., Rhodes, D. R., Perner, S., Dhanasekaran, S. M., Mehra, R., Sun, X. W., Varambally, S., Cao, X., Tchinda, J., Kuefer, R., Lee, C., Montie, J. E., Shah, R. B., Pienta, K. J., Rubin, M. A., and Chinnaiyan, A. M. Recurrent fusion of TMPRSS2 and ETS transcription factor genes in prostate cancer. Science, *310:* 644-648, 2005.

29. Singec, I., Knoth, R., Meyer, R. P., Maciaczyk, J., Volk, B., Nikkhah, G., Frotscher, M., and Snyder, E. Y. Defining the actual sensitivity and specificity of the neurosphere assay in stem cell biology. Nat Methods, *3:* 801-806, 2006.

30. Collins, A. T. and Maitland, N. J. Prostate cancer stem cells. Eur J Cancer, *42:* 1213-1218, 2006.

31. van Leenders, G. J., Aalders, T. W., Hulsbergen-van de Kaa, C. A., Ruiter, D. J., and Schalken, J. A. Expression of basal cell keratins in human prostate cancer metastases and cell lines. J Pathol, *195:* 563-570, 2001.

32. Bello-DeOcampo, D., Kleinman, H. K., Deocampo, N. D., and Webber, M. M. Laminin-1 and alpha6beta1 integrin regulate acinar morphogenesis of normal and malignant human prostate epithelial cells. Prostate, *46:* 142-153, 2001.

33. Shi, X., Gipp, J., and Bushman, W. Anchorage-independent culture maintains prostate stem cells. Dev Biol, *312:* 396-406, 2007.

34. Lang, S. H., Stower, M., and Maitland, N. J. In vitro modelling of epithelial and stromal interactions in non-malignant and malignant prostates. Br J Cancer, *82:* 990-997, 2000.

35. Gil-Diez de Medina, S., Salomon, L., Colombel, M., Abbou, C. C., Bellot, J., Thiery, J. P., Radvanyi, F., Van der Kwast, T. H., and Chopin, D. K. Modulation of cytokeratin subtype, EGF receptor, and androgen receptor expression during progression of prostate cancer. Hum Pathol, *29:* 1005-1012, 1998.

36. Lei, Q., Jiao, J., Xin, L., Chang, C. J., Wang, S., Gao, J., Gleave, M. E., Witte, O. N., Liu, X., and Wu, H. NKX3.1 stabilizes p53, inhibits AKT activation, and blocks prostate cancer initiation caused by PTEN loss. Cancer Cell, *9:* 367-378, 2006.

The Prostate

Patient Code	Age	Race	PSA	CA Locus	Grade	pStage
R060106	64	Asian	8	R,L,A,P	4+4	T2cNxMx
R060606	45	caucasian	4.8	RA,LB,LA	3+3	T2cNxMx
R061606	49	caucasian	NA	R	3+3	T2cNxMx
R062606	61	caucasian	NA	L	3+3	T2aNxMx
R071006	58	caucasian	NA	RA, RL.LL	3+3	T2cNxMx
R072406A	60	caucasian	NA	RA, RL	3+3	T3bNxMx
R072406B	69	hispanic	NA	RA, RL,LL	3+4	T2cNxMx
R072506	41	African-american	NA	R/L	3+4	T2cNxMx
R073106A	51	caucasian	3.5	R/L, A/P	3+3	T2cNxMx
R073106B	47	caucasian	NA	R/L,A/P	3+4	T2cN0Mx
R060106	64	Asian	8	R,L,A,P	4+4	T2cNxMx
D080406	69	caucasian	4.25	R/L, A/P	3+3	T2cN0MX
L081406	54	hispanic	NA	R/L	3+3	T2cN0MX
D082106	59	caucasian	3	LA	3+3	T2aN0Mx
R082606	51	African-american	NA	LA	3+3	T2aN0Mx
R091106	51	caucasian	2.75	R,L,A	3+3	T2cN0Mx
L091106	60	hispanic	19	R,L,A, A/P	3+4	T2cN0Mx
B100306	64	caucasian	6	R,L,A/P	3+3	T2cNoMx
D100606	67	caucasian	NA	Negative	Benign	NA
R100906	69	caucasian	NA	R,L,A/P	3+4	T2cNxMx
B100906	61	middle eastern	5	R,L,A/P	2+3	T2cN0Mx
L100906	60	caucasian	2.4	R,L	3+3	T2cN0Mx
D101606	66	caucasian	NA	L	3+4	T2aN0Mx
S101706	50	caucasian	5.41	R,L,A,P	3+3	T2cNxMx
S102306	64	caucasian	NA	Negative	Benign	NA
R103006	57	caucasian	NA	R	3+4	T2bNxMx
R103106	76	caucasian	NA	R,L,A/P,A	3+4	T2cnxMx
D110106	50	caucasian	75	R,L,A/P,A	4+3+5	T3aN0Mx
R110606	58	caucasian	NA	R,L,A/P,A	4+3+5	T2cNXMX
B011707	64	caucasian	4.3	R/L,A/P,B	3+3	T2cN0Mx
L030207	59	caucasian	5	R/L,A/P,B	3+4	T2cN0Mx
L030507	62	caucasian	5.4	R/L,A/P,	4+5	T3aN0Mx
S042307	58	caucasian	NA	R,L,A,P	4+3	T2cN0Mx
S050207	69	armenian	13	R,L,A,P	4+3	T3aN0Mx
D050207	70	caucasian	9.4	R,L,A,P	3+4	T2cN0Mx
R061807	61	caucasian	4.3	R,L	3+3	T3aNxMx
D080607	60	african-american	11	R	3+3	T2aN0Mx
R081307	62	caucasian	4.7	R,L	3+4	T2cNxMx
R091707	60	caucasian	3.9	R,L,A,P	3+3	T2cN0Mx
D092407	58	african-american	2.8	R,L	3+3	T2cN0Mx
R100107	67	caucasian	NA	R,L,A,P, Ap	3+3	T2cN0Mx
D100107	66	Asian	6.7	R	3+3	T2bN0Mx
R100807	51	caucasian	5.7	R,L, Ap	3+4	T2cN0Mx
D100807	76	caucasian	9	R,L,Mid,A	3+3	T2cN0MX
R102207	57	caucasian	4.6	R	3+3	T2aN0Mx

D111507	53	caucasian	4.1	R, P, Ap	3+3	T2aN0Mx
JR111907	73	caucasian	5	L, R, A, P	3+4	T2cN0Mx
R111907	69	caucasian	6.4	L,R,A,P	4+3	T2cNxMx
S120307	51	caucasian	8.5	R, A	3+4	T2aNxMx
S120907	54	caucasian	5.2	L,R,A,P	3+4	T2cNxMx
D121007	57	caucasian	1.8	L,R,A,P	4+5	T3aNoMx
R010708A	53	hispanic	9.5	L,P,Ap	3+4	T2cN0Mx
R010708B	51	caucasian	7.2	L,R,A,P,Ap	3+4	T2cNxMx
R011408	58	Asian	3.3	L,R,P,Ap	3+4	T2cNxMx
S011508	68	Asian	5.4	L,R,A,P,Ap	4+3	T2cNxMx
D012808A	58	caucasian	7.4	R,L,P	3+4	T2cNoMx
R020408	51	Hispanic	4.5	R,L,A,P	4+3	T2cNxMx
B021108	65	caucasian	5	R,L,A,P	3+4	T2cNoMx

Supplemental Table 1: Patients undergoing radical prostatectomy for prostate cancer were consented for tissue donation according to an approved protocol through the Office for the Protection of Research Subjects at UCLA. Patient information including age, pre-operative prostate specific antigen (PSA), tumor location on final pathology (R, Right, L, Left, A, Anterior, P, Posterior, Ap, Apex, B, Base), and pathological stage (T2, tumor confined within the prostatic capsule, T3, tumor extends beyond the prostate capsule) are shown in the table.

Supplemental Figure Legends:

Supplemental Figure 1: Formation of Prostaspheres in ULA plates. Specimens obtained from patients undergoing prostate surgery were mechanically and enzymatically digested. Single cells were and plated on ULA plates at high (10^5) or low (10^3) seeding density. Human prostaspheres developed within 1 week of seeding, however, aggregation occurred in the high-density cultures resulting in large spheroid aggregates (Figure 1A). Immunostaining for a variety of prostate markers of spheres generated in ULA cultures demonstrate a basal profile (1B).

Supplemental Figure 2: Analysis of cellular proliferation and apoptosis within human prostaspheres. Spheres were collected and paraffin-embedded after 10-21 days in culture. Ki-67 and TUNEL staining was used to evaluate cells undergoing proliferation or apoptosis. Ki-67 was consistently seen in the peripheral cells of the spheres. We were unable to detect apoptosis using the TUNEL assay. A positive control for TUNEL staining is shown in the lower left panel.

Supplemental Figure 3: Antigenic Marker Separation and Evaluation of Sphere-forming capability. Lin-CD44+ cells are enriched for sphere-forming capability.   A. Schematic diagram of cell fractionation based on surface marker expression using magnetic beads or automated cell sorting. B. FACS analysis of dissociated prostate cells subjected to enrichment/depletion of lineage, CD44, CD49f, or CD133 antigens.

Supplemental Figure 4: Trop-2 antibody staining demonstrates regenerated prostate tubules are of human origin. Immunostaining of regenerated human prostate tissue is performed using Goat anti-human trop-2 antibody (R&D Systems). Regenerated tissue using human prostate cells is shown in the upper panels and rodent tubules are shown in the lower panels. Only the human epithelial cells demonstrate Trop-2 expression when the anti-human antibody is utilized.

1
2
3
4
5
6
7
8
9
10
11
12
13
14
15
16
17
18
19
20
21
22
23
24
25
26
27
28
29
30
31
32
33
34
35
36
37
38
39
40
41
42
43
44
45
46
47
48
49
50
51
52
53
54
55
56
57
58
59
60

For Peer Review

1
2
3
4
5
6
7
8
9
10
11
12
13
14
15
16
17
18
19
20
21
22
23
24
25
26
27
28
29
30
31
32
33
34
35
36
37
38
39
40
41
42
43
44
45
46
47
48
49
50
51
52
53
54
55
56
57
58
59
60
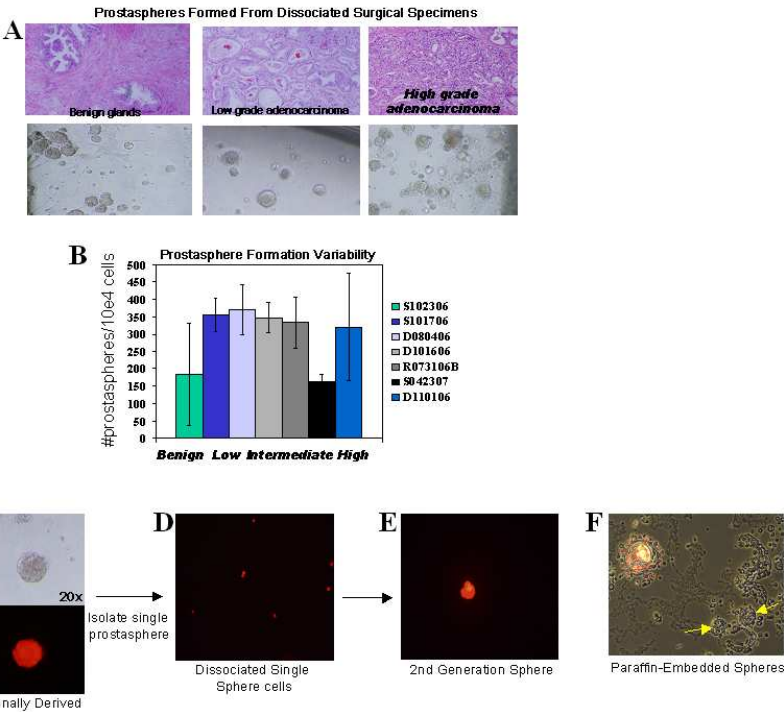
81x60mm (300 x 300 DPI)

Figure 2

81x60mm (300 x 300 DPI)

1
2
3
4
5
6
7
8
9
10
11
12
13
14
15
16
17
18
19
20
21
22
23
24
25
26
27
28
29
30
31
32
33
34
35
36
37
38
39
40
41
42
43
44
45
46
47
48
49
50
51
52
53
54
55
56
57
58
59
60
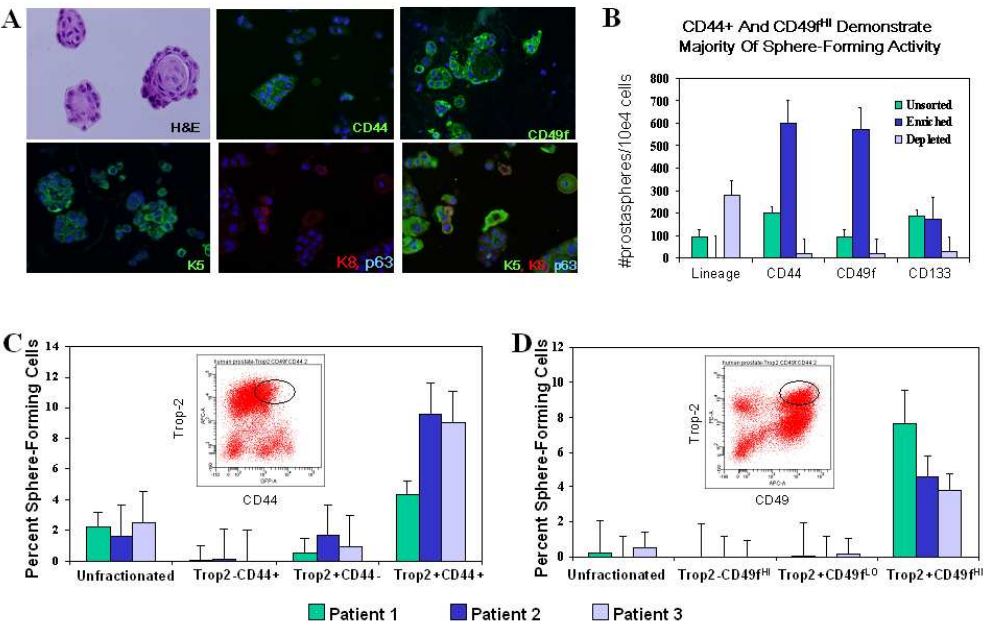
A

Patient Code	Age	CA Locus	Grade	pStage	TMPRSS2:ERG	FISH of Spheres
R072406A	60	RA, RL	3+3	T3bNxMx	Positive	Negative
R073106A	51	R/L, A/P	3+3	T2cNxMx	Positive	Negative
D110106	50	R, L, A/P, Ap	4+3+5	T3aN0Mx	Positive	Negative
R110606	58	R, L, A/P, Ap	4+3+5	T2cNxMx	Positive	Negative
B011707	64	R/L, A/P, B	3+3	T2cN0Mx	Positive	Negative
L030207	59	R/L, A/P, B	3+4	T2cN0Mx	Positive	Negative
L030507	62	R/L, A/P	4+5	T3aN0Mx	Positive	Negative

81x60mm (300 x 300 DPI)

Prostaspheres Induce Prostate Tissue Regeneration In Immunocompromised Mice

81x60mm (300 x 300 DPI)

81x60mm (300 x 300 DPI)

81x60mm (300 x 300 DPI)

1
2
3
4
5
6
7
8
9
10
11
12
13
14
15
16
17
18
19
20
21
22
23
24
25
26
27
28
29
30
31
32
33
34
35
36
37
38
39
40
41
42
43
44
45
46
47
48
49
50
51
52
53
54
55
56
57
58
59
60

A   Antigenic Marker
Separation Of Prostate Cells

Prostate tissue

Dissociated cells

Lineage Depletion
MACS beads column

FACS/Culture
Lin+ and Lin−
cells

Primary antibody (CD44, CD49f, or CD133)
MACS beads IgG column or cell sorting

FACS/Culture enriched and depleted fractions

B FACS Confirms Enrichment/Depletion Based On Antigenic Markers

Untreated   Lin depleted   CD44 depleted   CD44 enriched

CD45   CD44

CD 49f depleted   CD 49f enriched   CD133 depleted   CD133 enriched

0.45 %   10 %   0.38 %   34 %

CD133

81x60mm (300 x 300 DPI)

1
2
3
4
5
6
7
8
9
10
11
12
13
14
15
16
17
18
19
20
21
22
23
24
25
26
27
28
29
30
31
32
33
34
35
36
37
38
39
40
41
42
43
44
45
46
47
48
49
50
51
52
53
54
55
56
57
58
59
60

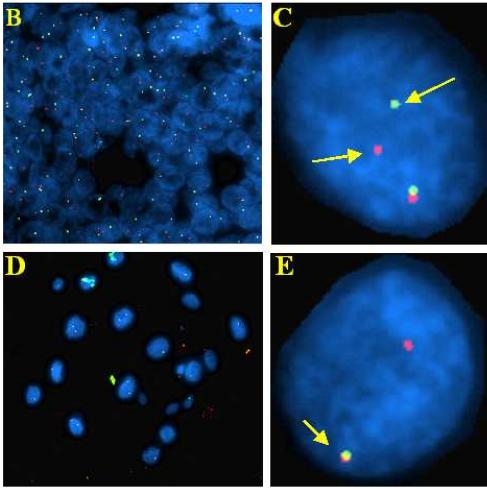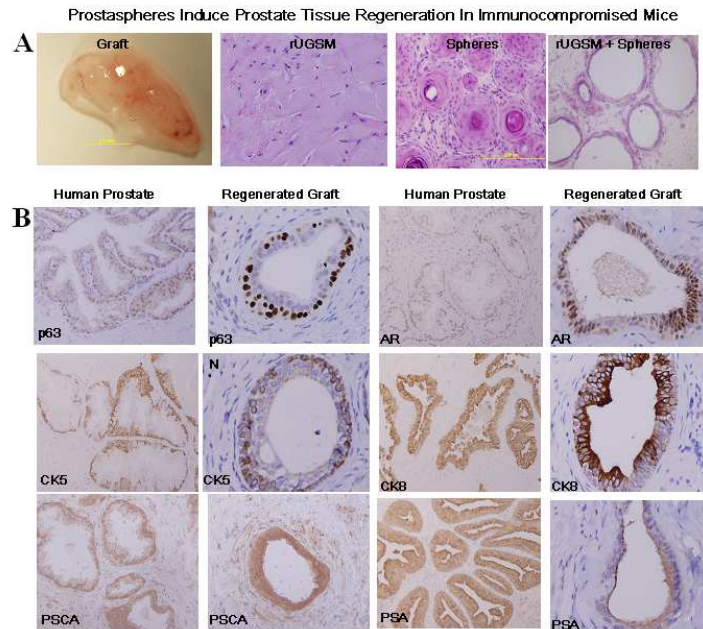**Membrane staining for human specific Trop2 antibody on human prostate regenerated structures but not mouse prostate regenerated structures demonstrates the species specificity**
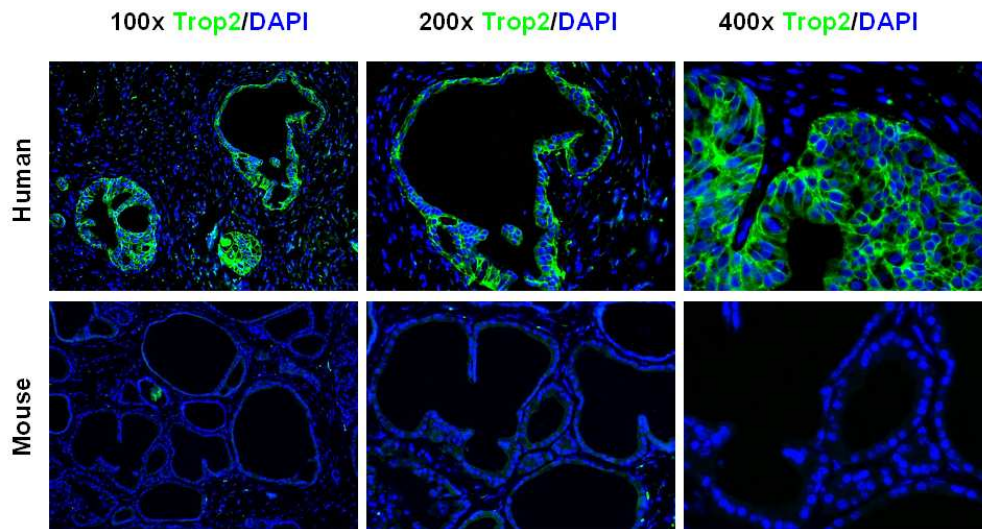
81x60mm (300 x 300 DPI)

Trop2 identifies a subpopulation of murine and human prostate basal cells with stem cell characteristics

Andrew S. Goldstein[a], Devon A. Lawson[b], Donghui Cheng[c], Wenyi Sun[d], Isla P. Garraway[d], and Owen N. Witte[a,b,c,e,f,1]

[a]Molecular Biology Institute, Departments of [b]Microbiology, Immunology, and Molecular Genetics, [d]Urology, and [e]Molecular and Medical Pharmacology, [c]Howard Hughes Medical Institute, David Geffen School of Medicine, and [f]Eli and Edythe Broad Center of Regenerative Medicine and Stem Cell Research, University of California, Los Angeles, CA 90095

The epithelium of the adult prostate contains 3 distinct cell types: basal, luminal, and neuroendocrine. Tissue-regenerative activity has been identified predominantly from the basal cells, isolated by expression of CD49f and stem cell antigen-1 (Sca-1). An important question for the field is whether all basal cells have stem cell characteristics. Prostate-specific microarray databases were interrogated to find candidate surface antigens that could subfractionate the basal cell population. Tumor-associated calcium signal transducer 2 (TACSTD2/Trop2/M1S1/GA733-1) was identified because it was enriched after castration, in prostate sphere cells and in the basal fraction. In the murine prostate, Trop2 shows progenitor characteristics such as localization to the region of the gland proximal to the urethra and enrichment for sphere-forming and colony-forming cells. Trop2 subfractionates the basal cells into 2 populations, both of which express characteristic basal cell markers by quantitative PCR. However, only the basal cells expressing high levels of Trop2 were able to efficiently form spheres in vitro. In the human prostate, where Sca-1 is not expressed, sphere-forming progenitor cells were also isolated based on high expression of Trop2 and CD49f. Trop2-expressing murine basal cells could regenerate prostatic tubules in vivo, whereas the remaining basal cells had minimal activity. Evidence was found for basal, luminal, and neuroendocrine cells in prostatic tubules regenerated from Trop2^{hi} basal cells. In summary, functionally distinct populations of cells exist within the prostate basal compartment and an epithelial progenitor can give rise to neuroendocrine cells in vivo.

neuroendocrine | progenitor | sphere assay

Many adult tissues of the body contain a rare population of somatic stem cells that can self-renew and differentiate into the mature cell types of the organ (1). Recent studies demonstrating that somatic stem cells can serve as the target for transforming mutations and act as cancer-initiating cells (2) have highlighted the importance of identifying tissue-specific stem cells. The isolation of somatic stem cells and subsequent investigation of their unique properties will be useful for understanding and targeting cancer.

The prostate epithelium is made up of basal, luminal, and neuroendocrine cells. Prostate stem cells are thought to reside within the basal layer because basal cells preferentially survive androgen ablation (3) and basal cells can give rise to luminal cells in vitro (4). The transcription factor p63 is expressed in prostate basal cells, and p63-null animals fail to develop a prostate (5). These data suggest that basal cells may represent or include prostate stem cells and that p63 may be essential for prostate development. However, the p63-null urogenital sinus epithelium forms prostatic tissue with luminal and neuroendocrine cells, but no basal cells (6). Both studies show that p63 plays an important developmental role in the prostate, but demonstrate conflicting data on the role of basal cells during differentiation. Based on expression of integrin $\alpha6$ (CD49f), Lawson *et al.* (7) found that the majority of cells in the gland with in vitro and in vivo

stem-like activity possessed basal cell characteristics. A fundamental question in the field is whether all basal cells have stem cell characteristics and can give rise to the mature cells of the organ or if only a subset of basal cells have tissue regenerative activity.

The neuroendocrine cell is the rarest epithelial cell type in the adult prostate. In the normal gland, neuroendocrine cells are dispersed within the basal layer (8) and extend processes between adjacent basal and luminal cells (9). Although their role in development and cancer is unclear, neuroendocrine cells are known to secrete neuropeptides that may contribute to hormone-refractory prostate cancer and metastasis through a paracrine mechanism (9–11). Neuroendocrine differentiation occurs in >30% of human prostate cancers (9) and in some mouse models of prostate cancer (12). However, studies correlating neuroendocrine differentiation and tumor grade have given conflicting results (9).

Evidence is lacking to definitively show whether neuroendocrine cells have an ectodermal or endodermal origin (13). Because of their location in the basal layer of prostatic tubules, neuroendocrine cells were believed to originate from an epithelial stem cell (endoderm). Human prostate epithelial progenitors can give rise to neuroendocrine-like cells in vitro (14, 15), and in response to a stimulus such as IL-6, LNCaP cells can adopt a neuroendocrine morphology and express high levels of neuronal markers (16).

An opposing theory is that neuroendocrine cells may have originated from the neural crest and migrated into the prostate epithelium. This theory is supported by the appearance of chromogranin A-positive cells in the embryonic site where the prostate forms, before gland formation, as demonstrated by Aumuller *et al.* (17). Cells expressing chromogranin A are first seen in the paraganglia flanking the mesenchyme and later in the urogenital mesenchyme. As the gland forms, chromogranin A-positive cells appear in the basal layer of the epithelium (17). However, the demonstration of neuroendocrine cells before prostatic gland formation does not exclude an epithelial origin for neuroendocrine cells found within the gland. In fact, neural crest derived cells may support the development of epithelial-derived neuroendocrine cells (9).

Leong *et al.* (18) recently demonstrated that enriched murine prostate stem cells could regenerate tissue grafts containing cells that express the neuroendocrine cell marker synaptophysin. The

presence of synaptophysin+ cells in grafts under the kidney capsule does not rule out neural crest-derived neuroendocrine cells migrating into prostatic tubules. Lineage tracing experiments are necessary to definitely determine whether epithelial progenitors can give rise to neuroendocrine cells in vivo.

The majority of markers used to isolate progenitors from the prostate are not conserved between mouse and human. In the human prostate, stem/progenitor cells have been enriched based on expression of integrins $\alpha2/\beta1$ (19), CD44 (20), or CD133 (21). Prostate stem/progenitor cells have been isolated from the mouse based on expression of stem cell antigen-1 (Sca-1) (22, 23), which is not expressed in the human prostate, and integrin $\alpha6$/CD49f (7, 24). In a recent report (18), murine prostate stem cells were also isolated by expression of CD44, CD133, and CD117. Leong *et al.* (18) note that CD117 is expressed in human prostate basal cells and may be a useful marker for isolating human prostate stem/progenitors. The identification of highly-enriched stem/progenitor populations in the mouse prostate is important for investigating the self-renewal properties of stem cells and their role in cancer initiation and propagation. However, the identification of stem/progenitor fractions from the human prostate has greater therapeutic implications. The cancer stem cell hypothesis suggests that a rare population of cancer cells may be responsible for sustaining tumorigenesis (1, 25–27) and these cancer stem cells often share antigenic profiles with normal tissue stem/progenitor cells (28, 29). These studies highlight the importance of identifying primitive cell populations from normal and malignant human prostate tissue, as new treatments may be designed to target cancer stem cells rather than the bulk tumor. Therefore, it would be useful to identify antigens found on stem/progenitor cells from both the mouse and human prostate.

We report the identification of a marker, tumor-associated calcium signal transducer 2 (TACSTD2/Trop2/M1S1/GA733-1) (30, 31), that functionally discriminates between 2 basal cell subpopulations. We demonstrate that not all basal cells share stem cell characteristics, and that basal cells expressing high levels of Trop2 are enriched for in vitro and in vivo stem-like activity. We follow the progeny of labeled cells to provide in vivo evidence that basal, luminal, and neuroendocrine cells are generated from an epithelial progenitor with tri-lineage differentiation potential. Finally, we show that sphere-forming progenitor cells can be isolated from the human prostate by using markers identified in the mouse (Trop2 and CD49f), suggesting a conservation of selected progenitor markers between mouse and human.

Results

Microarray Analysis Identifies Trop2 as a Candidate Progenitor Marker with Stem-Like Characteristics. We interrogated prostate-specific microarrays (from the literature and at the University of California, Los Angeles) where progenitor genes should be enriched to identify candidate antigens that may subfractionate prostate basal cells. We identified Trop2 as a leading candidate because it was 20-fold enriched in the murine prostate after castration (32), 12-fold enriched in prostate sphere cells compared with the total epithelium (Li Xin, Rita U. Lukacs, and O.N.W., unpublished work), and 2-fold enriched in the basal fraction compared with the remaining epithelium (Rita U. Lukacs, D.A.L., and O.N.W., unpublished work). Trop2 is a type I transmembrane protein in the EpCAM family with no known function or ligand (30, 31). Trop2 expression has been reported in normal and/or malignant tissue from kidney, lung, ovary, testis (33), intestine (34), pancreas (35), and breast (36); however, it has not been previously associated with stem or progenitor cells.

The putative prostate stem cell niche is found in the region closest to the urethra, referred to as the proximal region. Tsujimura *et al.* (37) used BrdU pulse–chase experiments to

Fig. 1. Trop2 has progenitor characteristics in the murine prostate. (*A*) Frozen prostate tissue sections from 8- to 12-week-old mice were stained with antibodies against Trop2 in combination with CD49f, cytokeratin 5, or cytokeratin 8. Sections were counterstained with DAPI (blue) nuclear stain. (*B*) FACS analysis for Trop2 on total dissociated prostate cells. (*C*) Trop2^{hi} and Trop2^{lo} prostate cells were isolated by FACS from 8- to 12-week-old mice. Cells were plated on top of a thin layer of Matrigel. Graph shows the colonies formed after 10 days versus the number of cells plated (1,000, 10,000). (*D*) Trop2^{hi} and Trop2^{lo} prostate cells were isolated by FACS from 8- to 12-week-old mice. Graph shows the spheres formed in Matrigel after 10 days versus the number of cells plated (1,000, 10,000).

demonstrate the majority of label retention in the proximal region of the gland and later showed that cells isolated from this region have higher proliferative capacity in vitro. To determine the expression pattern of Trop2 in the murine prostate, we used both FACS analysis and immunohistochemistry. FACS analysis demonstrates that Trop2 is highly expressed by $\approx$7–10% of the total prostate cells (Fig. 1*B*). Immunofluorescent staining on tissue sections revealed that Trop2 is expressed on cytokeratin 5+ (K5) basal cells and cytokeratin 8+ (K8) luminal cells in the proximal region, whereas almost no Trop2+ cells are found in the distal regions (Fig. 1*A*). In contrast, Trop2 is expressed on the majority of K5+ basal cells in the distal regions after androgen ablation (Fig. S1).

To investigate Trop2 as a functional progenitor marker, we turned to 2 in vitro assays that measure primitive cell activity: the prostate colony and sphere assays. Lawson and coworkers (7, 38) demonstrated that both colonies and spheres are clonal in origin, and the basal fraction contains the majority of colony-forming and sphere-forming cells. We isolated Trop2^{hi} and Trop2^{lo} cells by FACS and plated equal numbers of cells into the colony and sphere assays at 2 dilutions. The majority of colony-forming and sphere-forming activity was in the Trop2^{hi} fraction. Linear regression analysis demonstrates that Trop2^{hi} cells can form colonies at a rate of 1/38 and spheres at a rate of 1/58 (Fig. 1 *C* and *D*). Expressed on both basal and luminal cells, Trop2 identifies a progenitor population in the murine prostate with proximal localization and enrichment for in vitro activity in 2 independent assays indicative of primitive cell populations.

Trop2 Fractionates Lin$^-$Sca-1$^+$CD49f^{hi} Cells into Two Basal Subpopulations. We have previously demonstrated that the stem/ progenitor fraction defined by the antigenic profile CD45$^-$CD31$^-$Ter119$^-$Sca-1$^+$CD49f^{hi} (LSC) contains the majority of basal cells from the murine prostate (7). FACS analysis for Trop2 expression within the LSC fraction shows that Trop2 separates the basal cells into 2 relatively equal subpopulations,

MEDICAL SCIENCES

Fig. 2. Trop2 separates the Lin⁻Sca-1⁺CD49fʰⁱ fraction into 2 basal subpopu-lations. (*A*) FACS plots show gates drawn for sorting of Trop2ʰⁱ LSC (Lin⁻Sca-1⁺CD49fʰⁱ) and Trop2ˡᵒ LSC subpopulations from 8- to 12-week-old mice. (*B*) RNA was isolated from total cells, non-LSC (Lin⁻ not Sca-1⁺CD49fʰⁱ), Trop2ʰⁱ LSC, and Trop2ˡᵒ LSC fractions in duplicate experiments. RNA was synthesized into cDNA and subjected to qRT-PCR. Graph shows fold-enrichment over the total prostate cells for each gene. GAPDH was used as the reference gene.

and that ≈40% of LSC cells express high levels of Trop2 (Fig. 2*A*). We isolated RNA from these 2 populations (Trop2ʰⁱ LSC and Trop2ˡᵒ LSC) and the fraction depleted of LSC cells (non-LSC) and compared their gene expression with the total prostate. Quantitative RT-PCR (qRT-PCR) demonstrates that Trop2 is 6-fold enriched in the Trop2ʰⁱ LSC cells compared with the Trop2ˡᵒ fraction. Both populations express the basal markers p63, cytokeratins 5 and 14, and integrin α6 at high levels compared with the total prostate and the non-LSC cells (Fig. 2*B*). Nkx3.1 is not enriched in the LSC subpopulations, showing that the 2 fractions are depleted of mature markers. Based on these data, the Trop2ʰⁱ and Trop2ˡᵒ LSC cells have basal characteristics.

Trop2 and CD49f Enrich for Progenitors from the Mouse and Human Prostate. Having confirmed that Trop2 separates the basal fraction into 2 subpopulations that both express basal markers, we asked whether our basal subpopulations are functionally distinct. We isolated the LSC basal population and the further fractionated Trop2ʰⁱ and Trop2ˡᵒ basal subpopulations and plated equal cell numbers into the sphere assay. The LSC basal fraction formed spheres at a rate of 1/34, similar to what has been reported (7). The Trop2ʰⁱ basal fraction further enriched for sphere-forming cells to a frequency of 1/11, a 30-fold enrichment over the total unfractionated cells (1/330), whereas the Trop2ˡᵒ basal fraction only formed spheres at a rate of 1/132 (Fig. 3*A*). The residual sphere-forming activity in the Trop2ˡᵒ basal fraction may be explained by a small number of contaminating cells from the highly active Trop2ʰⁱ basal fraction. Alternatively, the Trop2ˡᵒ fraction may contain stem-like cells at a far lower frequency than the Trop2ʰⁱ fraction. Spheres from the Trop2ʰⁱ basal fraction could be passaged for >3 generations at a consistent rate of sphere formation to demonstrate self-renewal activity (primary: 1/11; passage 1: 1/10; passage 2: 1/10; passage 3: 1/8). Not only have we further refined the sphere-forming progenitor cell by using Trop2, but we have demonstrated that
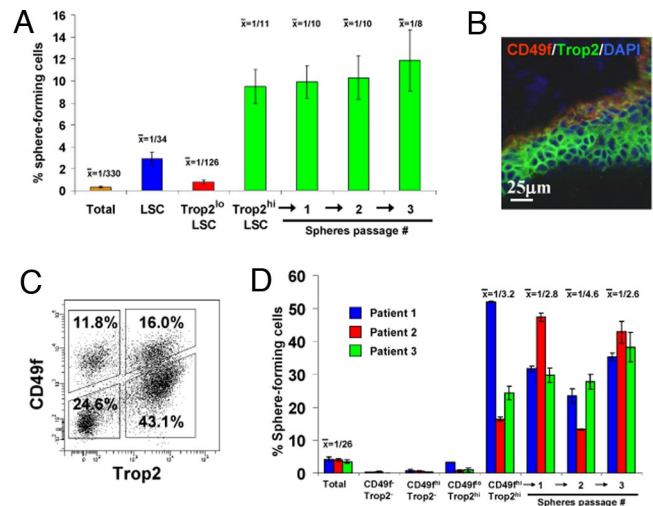
Fig. 3. Trop2 enriches for sphere-forming cells from the mouse and human prostate. (*A*) Total prostate, LSC, Trop2ʰⁱ LSC, and Trop2ˡᵒ LSC cells were isolated by FACS from 8- to 12-week-old mice. Graph shows the percentage of sphere-forming cells, based on the spheres formed in Matrigel from each population per 2,500 cells plated (5,000 cells plated from total prostate) after 8 days of growth. Spheres from the Trop2ʰⁱ LSC subpopulation were dissoci-ated and replated for 3 successive generations. Data from several experiments were pooled. (*B*) Frozen human prostate tissue sections were stained with antibodies against Trop2 and CD49f. Sections were counterstained with DAPI (blue) nuclear stain. (*C*) FACS plots show gates drawn for sorting of human prostate cells into 4 subpopulations based on expression of Trop2 and CD49f. (*D*) Total prostate, CD49f⁻Trop2⁻, CD49fʰⁱTrop2⁻, CD49fˡᵒTrop2ʰⁱ, and CD49fʰⁱTrop2ʰⁱ subpopulations were isolated by FACS from 3 patient samples. Graph shows the percentage of sphere-forming cells, based on the spheres formed in Matrigel from each population per 2,500 cells plated after 7 days of growth. Spheres from the CD49fʰⁱTrop2ʰⁱ subpopulation were dissociated and passaged for 3 successive generations.

the majority of stem-like activity is contained within a subpopu-lation of basal cells.

Similar to the prostate sphere assay described in the mouse system (38), primary human prostate cells can form spheres in Matrigel that demonstrate progenitor characteristics, such as self-renewal in vitro and differentiation to the basal and luminal cell types in vivo. Human prostaspheres are clonally derived and predominantly express basal markers. When a mixture of ma-lignant cells with a TMPRSS2-ERG translocation and normal cells (without the translocation) are plated into the assay, the resulting spheres do not retain the translocation, suggesting that the assay selects for normal progenitors (I.P.G., C. Tran, S. Perner, W.S., B. Zhang, L. Xin, C. Head, R. Reiter, M. Rubin, and O.N.W., unpublished work).

Having demonstrated that we can enrich for murine prostate sphere-forming cells by using Sca-1, CD49f, and Trop2, we looked to identify the human prostate sphere-forming cell. Although Sca-1 is not expressed in the human prostate, we found expression of both Trop2 and CD49f. In tissue sections, the highest expression of Trop2 and CD49f is observed along the basal layer of the epithelium (Fig. 3*B*). FACS analysis shows that Trop2 and CD49f separate the human prostate into 4 popula-tions (Fig. 3*C*). We collected prostate tissue from multiple patients who underwent prostate removal for cancer. Human prostate tissue specimens were mechanically and enzymatically dissociated into single cells and cultured overnight in serum-free media. Dissociated cells were sorted into 4 populations based on CD49f and Trop2, and equal cell numbers were plated into the sphere assay. Data for 3 representative patients are shown, and the results have been repeated for all patients that have been analyzed (data not shown). The overnight culture enriched for

progenitor cells before antigen separation, as the total population sent through the sorter formed spheres at an average rate of 1/26. Upon fractionating the cells, the majority of sphere-forming activity came from the cells expressing high levels of CD49f and Trop2, as seen in the mouse. Cells from the CD49f^{hi}Trop2^{hi} population comprised ≈16% of the total prostate cells after short-term culturing, and this fraction formed spheres at an average rate of 1/3.2, an 8-fold enrichment over the total unfractionated cells (Fig. 3D). Spheres from this enriched fraction could be passaged for up to 3 generations at a sphere-forming rate similar to the original CD49f^{hi}Trop2^{hi} fraction (primary: 1/3.2; passage 1: 1/2.8; passage 2: 1/4.6; passage 3: 1/2.6). Our data show that we can reproducibly isolate sphere-forming progenitor cells from the human prostate by using markers that were identified in the murine prostate, suggesting a conservation of progenitor markers that may be found in other epithelial tissues.

Trop2^{hi} Basal Cells Give Rise to Basal, Luminal, and Neuroendocrine Cells in Vivo. Previous experiments showed that the Lin^{−}Sca-1^{+}CD49f^{hi} basal fraction could produce prostatic tubules when combined with urogenital sinus mesenchyme (UGSM) and implanted s.c. into immunodeficient mice with Matrigel (7). Regenerated tubules contained basal and luminal cells, but neuroendocrine cells were not evaluated. Recently, neuroendocrine cells were found in tissue regenerated from Lin^{−}Sca-1^{+}CD133^{+}CD44^{+}CD117^{+} cells (18); however, experiments were not performed to demonstrate a definitive epithelial origin. To follow the progeny of implanted stem cells, we used transgenic mice expressing either GFP or DsRed under the β-actin promoter. Fluorescently-labeled DsRed[+] Trop2^{hi} and Trop2^{lo} basal cells were isolated from β-actin-DsRed mice and combined with 10[5] total unfractionated GFP^{+} prostate cells from β-actin–GFP mice. Purified DsRed[+] and total GFP^{+} cells were combined with 2 × 10^{5} UGSM cells and implanted s.c. into SCID mice. After 8 weeks of growth, we harvested grafts and looked for fluorescently-labeled prostatic tubules. We found that whereas all grafts contained an abundance of GFP[+] tubules (Fig. 4A2), the Trop2^{hi} basal fraction gave rise to the majority of DsRed[+] prostatic tubules (Fig. 4A3). Previous experiments performed without total unfractionated cells yielded similar results at a lower frequency of tubule formation (data not shown).

Analysis of sectioned tubules revealed K5+ and p63+ basal cells and K8+ luminal cells. Androgen receptor was detected primarily in luminal cells (Fig. 4 B 5 and 6). In addition to the basal and luminal cells that were previously detected in regenerated tissue, we found rare cells within the basal layer of DsRed[+] tubules that expressed the neuroendocrine marker synaptophysin (Fig. 4B7). The membrane localization and extended morphology of regenerated synaptophysin+ cells appeared similar to those found in synaptophysin+ neuroendocrine cells from the adult murine prostate (Fig. 4B8). Within the basal layer of regenerated tubules, we found numerous examples of synaptophysin+ cells extending dendrite-like processes around neighboring epithelial cells (Fig. 4B 9–12), characteristic of neuroendocrine morphology. To quantify the frequency of neuroendocrine cells, we detected an average of 6 synaptophysin+ cells per 66 regenerated tubules in a 4-μm thick tissue section (18 sections counted). In normal prostate tissue sections, many of the synaptophysin+ cells also expressed chromogranin A. We were unable to demonstrate chromogranin A reactivity in regenerated tissue sections, suggesting a lack of full neuroendocrine differentiation. Factors from the native prostatic niche that support neuroendocrine development may be absent in the assay microenvironment. Alternatively, full neuroendocrine differentiation may take longer than the 8-week regeneration process.

Because evidence suggests that prostate neuroendocrine cells
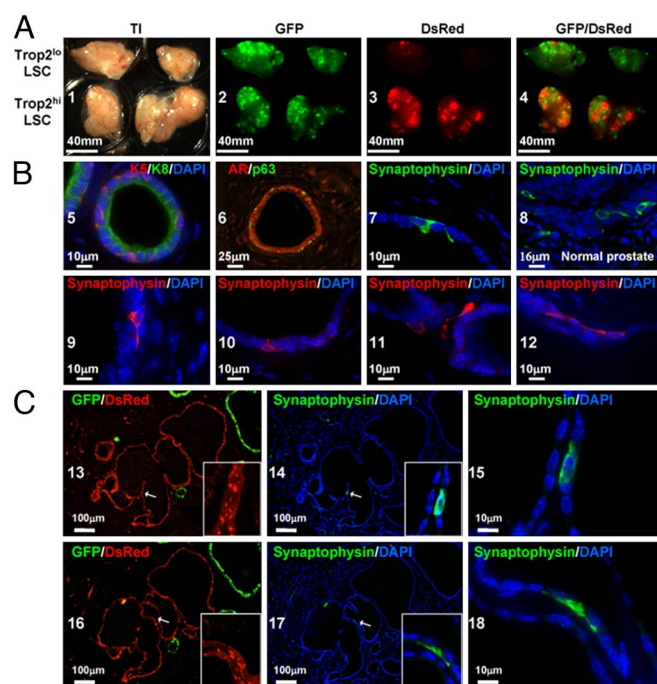
Fig. 4. Trop2^{hi} LSC cells give rise to basal, luminal, and neuroendocrine cells in vivo. (A) A total of 3 × 10^{3} Trop2^{hi} LSC or Trop2^{lo} LSC cells from β-actin DsRed mice, 10[5] total prostate cells from β-actin GFP mice, and 2 × 10^{5} UGSM cells were combined in Matrigel and injected s.c. into SCID mice. Grafts were harvested after 8 weeks, and overview images were taken by using transillumination (TI) and DsRed or GFP fluorescence. (B) Tissue sections from regenerated tissue were stained for antibodies against cytokeratin 5 (K5), cytokeratin 8 (K8), androgen receptor (AR), p63, and synaptophysin. Sections were counterstained with DAPI (blue) nuclear stain. Sections from 8- to 12-week-old mice were stained for comparison of neuroendocrine cell morphology and marker expression pattern (synaptophysin). (C) In tissue sections from regenerated tissue, DsRed and GFP fluorescence (13 and 16) were visualized before antigen retrieval caused by a loss of signal after treatment. The remaining images demonstrate synaptophysin staining and DAPI nuclear counterstain after antigen retrieval.

have an ectodermal/neural crest origin (17), we looked for synaptophysin+ cells within DsRed+ tubules to demonstrate an epithelial origin for neuroendocrine cells. Only cells derived from the Trop2^{hi} LSC stem/progenitor fraction should express DsRed fluorescence. If neuroendocrine cells migrate into the regenerated tubules from an alternate location, they should not express DsRed. We identified neuroendocrine cells within the basal layer of regenerated tubules with characteristic neuroendocrine morphology (Fig. 4B 15 and 18) that colocalize with DsRed fluorescence (Fig. 4B 13, 14, 16, and 17). By following the progeny of DsRed+ Trop2^{hi} basal cells into DsRed+ synaptophysin+ neuroendocrine cells, we have provided direct evidence that a prostate stem cell can generate 3 epithelial cell types.

Discussion

Stem cells isolated from different epithelial tissues share antigenic profiles, such as integrins α6 and β1, the stem cell antigen Sca-1, and CD24 (7, 39, 40). Similarly, somatic and cancer stem cells have been isolated from numerous human tissues by using the markers CD44 and CD133 (19, 21, 26, 27). We have found 2 markers, Trop2 and CD49f, which are conserved between mouse and human. Because of the similarity of stem cell profiles, the identification of markers such as Trop2 should be useful for multiple tissue systems.

In the mouse prostate, we have shown that a subpopulation of basal cells, expressing high levels of Trop2, have stem cell

MEDICAL SCIENCES

characteristics. It is unlikely that the spheres and tubules generated by Trop2^{hi} basal cells are different from those generated in previously published studies. We have simply enriched for the cells capable of generating these structures. Although we have now identified neuroendocrine cells and traced their lineage from epithelial progenitors, the purification of stem-like cells is not necessary to regenerate tissue containing neuroendocrine cells. Using different immunohistochemical techniques and antibodies, we can now detect neuroendocrine cells in grafts generated from unfractionated cells (data not shown).

Although Trop2^{hi} basal cells can efficiently form spheres and tubules, the remaining basal cells have minimal activity in vitro and in vivo. Both of these populations express high levels of CD49f and other basal cell genes, but they differ in their functional output. This finding has interesting implications for the epithelial lineage hierarchy in the prostate. Linear models of prostate differentiation have suggested that stem cells in the basal layer give rise to transit-amplifying cells that differentiate into mature luminal cells (14, 41). In our assays, all basal cells do not have stem cell activity. Our data support an alternative branching model, where a subset of basal cells can differentiate into basal, luminal, and neuroendocrine cells. A similar model has been reported in the mammary system, where stem cells give rise to both basal/myoepithelial and luminal progenitors, which differentiate into mature basal and luminal cells. Future identification of a luminal progenitor, as demonstrated in the mammary system (42), would further support the branching model.

Trop2 is highly expressed by a subset of both basal (30–40% Trop2^{hi}) and luminal (5–15% Trop2^{hi}) cells in the murine prostate (Fig. 2A and data not shown). Trop2^{hi} cells are concentrated in the proximal region, the putative prostate stem cell niche. We observed a similar region-restricted expression pattern in murine endometrial glands, where the brightest Trop2 staining was observed in regions of invagination (Fig. S2). The restricted pattern suggests that a localized niche signal, such as the Wnt pathway, may control Trop2 expression. Segditsas *et al.* (43) showed that Trop2 has high confidence TCF4 binding sites and may be a Wnt target gene in the intestinal epithelium. Trop2 was significantly enriched in early intestinal cancers driven by APC mutations as compared with the normal tissue. A similar pattern was seen with the crypt stem cell marker Lgr5 (Gpr49) and other Wnt target genes (43).

We also found that Trop2 expression is significantly increased during tumorigenesis caused be aberrant PI3K signaling. Thirty-three percent of cells from Pten-null murine prostate tumors were Trop2^{hi} by FACS analysis compared with ≈8% in aged-matched wild-type prostate tissue (Fig. S3). A conserved mechanism in multiple organ systems could regulate Trop2 expression in the normal and malignant niche. Although the function of Trop2 in normal and cancer cells has yet to be elucidated, Trop2 appears to play a role in the tumorigenicity and invasion of cancer cells. Targeting Trop2 in colon cancer cells through RNA interference reduces both soft-agar colony formation and tumor initiation in mice, whereas inhibitory antibodies can block invasion in Matrigel in vitro (44). Trop2 may also have oncogenic activity through a chimeric CYCLIN D1-TROP2 mRNA present in many human cancers (45). The cancer stem cell marker EpCAM (26), a Trop2 family member, is a therapeutic target in a variety of epithelial cancers and likely contributes to oncogenic signaling beyond cell–cell adhesion (46). Trop2 and EpCAM may have similar functions in solid tumors.

Our demonstration that only a subpopulation of basal cells has stem cell characteristics raises some interesting questions about the cell of origin for prostate cancer. Can both basal subpopulations give rise to prostate cancer, or are the more primitive cells the preferred target for transforming mutations that drive tumorigenesis? Can different genetic and epigenetic changes lead to cancer initiation from different basal subpopulations?

The finding that prostate stem cells can give rise to basal, luminal, and neuroendocrine cells, and the fact that the majority of human prostate tumors have a predominant luminal phenotype (47) and focal neuroendocrine differentiation (48) supports the theory that prostate cancer can initiate from a progenitor with luminal and neuroendocrine differentiation potential.

Recent reports on the role of stem cells in the initiation and propagation of cancer suggest that it may be important to target prostate cancer at the level of the stem cell (2, 28, 29). Defining and profiling these 2 basal subpopulations should elucidate the mechanisms by which the more primitive basal cells maintain their self-renewal and differentiation potential. The identification of critical self-renewal mechanisms in Trop2^{hi} basal cells may provide new targets for the treatment of prostate cancer.

Materials and Methods

Animals and Tissue Collection. The wild-type C57BL/6, β-actin GFP (C57BL/6-Tg[ACTbEGFP]1Osb), β-actin DsRed (C57BL/6-Tg[ACTB-DsRed.MST]1Nagy/J), and CB17$^{Scid/Scid}$ mouse strains were purchased from The Jackson Laboratory. Mice were housed and bred under the regulation of the Division of Laboratory Animal Medicine at the University of California, Los Angeles. Prostate cell dissociation was adapted from previously described protocols (49). Prostate tissue was collected from 8- to 12-week-old mice, minced into small fragments, digested with collagenase (GIBCO) as described (49), and digested with 0.05% trypsin/EDTA (Invitrogen) for 5 min at 37 °C. The cell suspension was passed through 18- to 22-gauge syringes several times and filtered through a 40-μm cell strain. UGSM was harvested as described (49).

Immunofluorescent and Histological Analysis. Immunohistochemical analysis of frozen and paraffin-embedded tissue sections were performed as described (7, 49). Antibodies are listed in *SI Text*. Sections were counterstained with DAPI (Vector) and analyzed by fluorescent microscopy.

FACS. Dissociated prostate cells were suspended in DMEM/10% FBS and stained with antibody for 30 min at 4 °C. Antibodies are listed in *SI Text*. FACS analysis was performed by using BD FACS Canto (BD Biosciences). Cell sorting was done by using BD FACS Vantage and the BD FACS Aria II.

In Vitro Prostate Colony- and Sphere-Forming Assays. The colony assay was adapted from previously described protocols (7). Isolated epithelial cells were plated on top of a thin layer of Matrigel (BD Biosciences), rather than on irradiated feeder cells. The sphere assay was performed as described (7, 38).

In Vivo Prostate Regeneration. Dissociated or FACS-isolated prostate cells were counted by hemocytometer and mixed with 2×10^5 UGSM cells as described (7). Cell mixtures were pelleted, resuspended in 40 μL of Matrigel (kept on ice), and injected s.c. on the backs of 8-to 16-week-old CB17$^{Scid/Scid}$ mice by using an insulin syringe. Eight weeks later, grafts were harvested, sectioned, and stained.

RNA Isolation and qRT-PCR. Sorted cells were collected, spun down, and resuspended in buffer RLT from the RNeasy Micro Kit (Qiagen). The standard RNA isolation protocol was followed. Reverse transcription was performed with a SuperScript III first-strand synthesis system (Invitrogen). qRT-PCR was performed by using iQ SYBR Green Supermix for Real-Time PCR (Bio-Rad) on a Bio-Rad iCycler and iQ5 2.0 Standard Edition Optical System Software. Data were analyzed by using the Pfaffl method. Primer sequences are listed in Table S1.

Human Prostate Tissue Acquisition and Dissociation. Human prostate tissue was obtained from 3 patients undergoing retropubic prostatectomy for adeno-carcinoma of the prostate or cystoprostatectomy for bladder cancer. All subjects provided consent for tissue collection in accordance with an approved protocol through the office for the protection of research subjects at the University of California, Los Angeles. Tissue specimens were placed on ice and brought immediately to the laboratory for mechanical and enzymatic digestion. Prostate tissue was sharply minced into small fragments (1 mm³) in RPMI-1640 medium supplemented with 10% FBS. Tissue fragments were washed once and incubated for 12 h in 0.25% type I collagenase (5 mL/g). Organoids were washed in RPMI-1640 medium and treated with TripLE (Invitrogen) for 5 min at 37 °C. Dissociated tissue cellular suspensions were sequentially filtered through 100- and 40-μm filters. After filtration, cell suspensions were passed through a 23-gauge needle. Cells were plated overnight in PrEGM (Clonetics).

1. Reya T, Morrison SJ, Clarke MF, Weissman IL (2001) Stem cells, cancer, and cancer stem cells. *Nature* 414:105–111.
2. Passegue E, Wagner EF, Weissman IL (2004) JunB deficiency leads to a myeloproliferative disorder arising from hematopoietic stem cells. *Cell* 119:431–443.
3. English HF, Santen RJ, Isaacs JT (1987) Response of glandular versus basal rat ventral prostatic epithelial cells to androgen withdrawal and replacement. *Prostate* 11:229–242.
4. Robinson EJ, Neal DE, Collins AT (1998) Basal cells are progenitors of luminal cells in primary cultures of differentiating human prostatic epithelium. *Prostate* 37:149–160.
5. Signoretti S, et al. (2000) p63 is a prostate basal cell marker and is required for prostate development. *Am J Pathol* 157:1769–1775.
6. Kurita T, Medina RT, Mills AA, Cunha GR (2004) Role of p63 and basal cells in the prostate. *Development* 131:4955–4964.
7. Lawson DA, Xin L, Lukacs RU, Cheng D, Witte ON (2007) Isolation and functional characterization of murine prostate stem cells. *Proc Natl Acad Sci USA* 104:181–186.
8. Abate-Shen C, Shen MM (2000) Molecular genetics of prostate cancer. *Genes Dev* 14:2410–2434.
9. Abrahamsson PA (1999) Neuroendocrine differentiation in prostatic carcinoma. *Prostate* 39:135–148.
10. Chuang CK, Wu TL, Tsao KC, Liao SK (2003) Elevated serum chromogranin A precedes prostate-specific antigen elevation and predicts failure of androgen deprivation therapy in patients with advanced prostate cancer. *J Formos Med Assoc* 102:480–485.
11. Uchida K, et al. (2006) Murine androgen-independent neuroendocrine carcinoma promotes metastasis of human prostate cancer cell line LNCaP. *Prostate* 66:536–545.
12. Chiaverotti T, et al. (2008) Dissociation of epithelial and neuroendocrine carcinoma lineages in the transgenic adenocarcinoma of mouse prostate model of prostate cancer. *Am J Pathol* 172:236–246.
13. Matusik RJ, et al. (2008) Prostate epithelial cell fate. *Differentiation* 76:682–698.
14. Litvinov IV, et al. (2006) Low-calcium serum-free defined medium selects for growth of normal prostatic epithelial stem cells. *Cancer Res* 66:8598–8607.
15. Rumpold H, et al. (2002) Neuroendocrine differentiation of human prostatic primary epithelial cells in vitro. *Prostate* 53:101–108.
16. Qiu Y, Robinson D, Pretlow TG, Kung HJ (1998) Etk/Bmx, a tyrosine kinase with a pleckstrin-homology domain, is an effector of phosphatidylinositol 3′-kinase and is involved in interleukin-6-induced neuroendocrine differentiation of prostate cancer cells. *Proc Natl Acad Sci USA* 95:3644–3649.
17. Aumuller G, et al. (1999) Neurogenic origin of human prostate endocrine cells. *Urology* 53:1041–1048.
18. Leong KG, Wang BE, Johnson L, Gao WQ (2008) Generation of a prostate from a single adult stem cell. *Nature*, in press.
19. Collins AT, Habib FK, Maitland NJ, Neal DE (2001) Identification and isolation of human prostate epithelial stem cells based on α(2)β(1)-integrin expression. *J Cell Sci* 114:3865–3872.
20. Collins AT, Berry PA, Hyde C, Stower MJ, Maitland NJ (2005) Prospective identification of tumorigenic prostate cancer stem cells. *Cancer Res* 65:10946–10951.
21. Richardson GD, et al. (2004) CD133, a novel marker for human prostatic epithelial stem cells. *J Cell Sci* 117:3539–3545.
22. Burger PE, et al. (2005) Sca-1 expression identifies stem cells in the proximal region of prostatic ducts with high capacity to reconstitute prostatic tissue. *Proc Natl Acad Sci USA* 102:7180–7185.
23. Xin L, Lawson DA, Witte ON (2005) The Sca-1 cell surface marker enriches for a prostate-regenerating cell subpopulation that can initiate prostate tumorigenesis. *Proc Natl Acad Sci USA* 102:6942–6947.
24. Goto K, et al. (2006) Proximal prostatic stem cells are programmed to regenerate a proximal-distal ductal axis. *Stem Cells* 24:1859–1868.
25. Al-Hajj M, Wicha MS, Benito-Hernandez A, Morrison SJ, Clarke MF (2003) Prospective identification of tumorigenic breast cancer cells. *Proc Natl Acad Sci USA* 100:3983–3988.
26. Dalerba P, et al. (2007) Phenotypic characterization of human colorectal cancer stem cells. *Proc Natl Acad Sci USA* 104:10158–10163.
27. Singh SK, et al. (2004) Identification of human brain tumor-initiating cells. *Nature* 432:396–401.
28. Ginestier C, et al. (2007) ALDH1 is a marker of normal and malignant human mammary stem cells and a predictor of poor clinical outcome. *Cell Stem Cell* 1:555–567.
29. Malanchi I, et al. (2008) Cutaneous cancer stem cell maintenance is dependent on β-catenin signaling. *Nature* 452:650–653.
30. Fornaro M, et al. (1995) Cloning of the gene encoding Trop-2, a cell-surface glycoprotein expressed by human carcinomas. *Int J Cancer* 62:610–618.
31. Tsujikawa M, et al. (1999) Identification of the gene responsible for gelatinous drop-like corneal dystrophy. *Nat Genet* 21:420–423.
32. Wang XD, et al. (2007) Expression profiling of the mouse prostate after castration and hormone replacement: Implication of H-cadherin in prostate tumorigenesis. *Differentiation* 75:219–234.
33. El Sewedy T, Fornaro M, Alberti S (1998) Cloning of the murine TROP2 gene: Conservation of a PIP2-binding sequence in the cytoplasmic domain of TROP-2. *Int J Cancer* 75:324–330.
34. Ohmachi T, et al. (2006) Clinical significance of TROP2 expression in colorectal cancer. *Clin Cancer Res* 12:3057–3063.
35. Fong D, et al. (2008) High expression of TROP2 correlates with poor prognosis in pancreatic cancer. *Br J Cancer* 99:1290–1295.
36. Huang H, et al. (2005) Aberrant expression of novel and previously described cell membrane markers in human breast cancer cell lines and tumors. *Clin Cancer Res* 11:4357–4364.
37. Tsujimura A, et al. (2002) Proximal location of mouse prostate epithelial stem cells: A model of prostatic homeostasis. *J Cell Biol* 157:1257–1265.
38. Xin L, Lukacs RU, Lawson DA, Cheng D, Witte ON (2007) Self-renewal and multilineage differentiation in vitro from murine prostate stem cells. *Stem Cells* 25:2760–2769.
39. Shackleton M, et al. (2006) Generation of a functional mammary gland from a single stem cell. *Nature* 439:84–88.
40. Stingl J, et al. (2006) Purification and unique properties of mammary epithelial stem cells. *Nature* 439:993–997.
41. Lawson DA, Witte ON (2007) Stem cells in prostate cancer initiation and progression. *J Clin Invest* 117:2044–2050.
42. Asselin-Labat ML, et al. (2007) Gata-3 is an essential regulator of mammary-gland morphogenesis and luminal-cell differentiation. *Nat Cell Biol* 9:201–209.
43. Segditsas S, et al. (2008) Putative direct and indirect Wnt targets identified through consistent gene expression changes in APC-mutant intestinal adenomas from humans and mice. *Hum Mol Genet* 17:3864–3875.
44. Wang J, Day R, Dong Y, Weintraub SJ, Michel L (2008) Identification of Trop-2 as an oncogene and an attractive therapeutic target in colon cancers. *Mol Cancer Ther* 7:280–285.
45. Guerra E, et al. (2008) A bicistronic CYCLIN D1-TROP2 mRNA chimera demonstrates a novel oncogenic mechanism in human cancer. *Cancer Res* 68:8113–8121.
46. Baeuerle PA, Gires O (2007) EpCAM (CD326) finding its role in cancer. *Br J Cancer* 96:417–423.
47. Okada H, et al. (1992) Keratin profiles in normal/hyperplastic prostates and prostate carcinoma. *Virchows Arch A Pathol Anat Histopathol* 421:157–161.
48. di Sant'Agnese PA (1992) Neuroendocrine differentiation in human prostatic carcinoma. *Hum Pathol* 23:287–296.
49. Xin L, Ide H, Kim Y, Dubey P, Witte ON (2003) In vivo regeneration of murine prostate from dissociated cell populations of postnatal epithelia and urogenital sinus mesenchyme. *Proc Natl Acad Sci USA* 100:11896–11903.

MEDICAL SCIENCES

Direct transformation of primary human prostate epithelial cells

Andrew S. Goldstein[1], Jiaoti Huang[3], Changyong Guo[2,4], Isla P. Garraway[2,4], Owen N. Witte[1,5,6,7,8]

[1]Molecular Biology Institute, [2]Jonsson Comprehensive Cancer Center, Departments of [3]Pathology and Laboratory Medicine, [4]Urology, [5]Microbiology, Immunology and Molecular Genetics, [6]Molecular and Medical Pharmacology, [7]Howard Hughes Medical Institute, David Geffen School of Medicine, and [8]Eli and Edythe Broad Center of Regenerative Medicine and Stem Cell Research, University of California, Los Angeles, CA 90095

Corresponding Author: Owen N. Witte, M.D.

Howard Hughes Medical Institute

University of California, Los Angeles

675 Charles E. Young Dr. South

5-748 MRL

Los Angeles, CA 90095-1662

Phone: 310-206-0386

FAX: 310-206-8822

Email: owenwitte@mednet.ucla.edu

Epithelial cell transformation has been demonstrated in numerous animal models for the study of solid tumor biology. However, little evidence exists for human epithelial cell transformation without prior immortalization[1], limiting our knowledge of the events that can transform naïve human epithelium. Prostate cancer research has been hindered by an absence of human tissue model systems that can recapitulate tumorigenesis[2]. Here we demonstrate direct transformation of freshly-isolated primary human prostate epithelial cells without prior culture or immortalization. The cooperative effects of two of the most common alterations in human prostate cancer, PI3K pathway activation and increased expression of the ETS transcription factor ERG[3-5], were capable of initiating high grade PIN (prostatic intraepithelial neoplasia) lesions from basal cells but not luminal cells. Basal-derived lesions demonstrate morphologic and molecular features of malignant transformation, including differentiation to tubular structures with an expansion of luminal cells expressing AR (androgen receptor) and PSA (prostate-specific antigen). We present a highly malleable system to demonstrate the direct conversion of primary benign human cells to a malignant phenotype. Our results show that basal cells can serve as one cell-of-origin for human prostate cancer.

The *in vivo* human prostate epithelial hierarchy and the cell-of-origin for human prostate cancer, two central issues to cancer biology, have remained elusive. The prostate epithelium is comprised primarily of basal and luminal cells, with rare neuroendocrine cells. Interestingly, prostate-regenerating stem cell activity has been demonstrated from

both basal and luminal cells using *in vivo* mouse models[6-8]. While human prostate basal cells can differentiate into AR+/PSA+ luminal-like cells *in vitro*[9] and generate rare acinar structures *in vivo*[10], a robust human prostate-regeneration assay is necessary to determine the *in vivo* epithelial hierarchy. Our approach was to purify basal and luminal epithelial cells from freshly-isolated human prostate tissue and compare their stem cell activity and cancer-initiating activity using an *in vivo* prostate-regeneration and direct transformation assay.

No commonly accepted strategy exists to isolate both basal and luminal cells from dissociated human prostate tissue. We have previously demonstrated expression of CD49f (integrin alpha 6) and Trop2 (TACSTD2) in human prostate tissue by immunohistochemical staining and flow cytometry, where these two antigens distinguish four separate populations[6] (Fig. 1a). We have now performed gene expression analysis on these four populations with a focus on genes characteristic of basal cells, luminal cells and non-epithelial cells. The CD49f^{hi}Trop2^{hi} fraction, previously demonstrated to possess sphere-forming activity *in vitro*[6], is enriched for the basal keratins 5 and 14 and the basal transcription factor p63 (Fig. 1e-g). The CD49f^{lo}Trop2^{hi} population expresses high levels of luminal-enriched genes such as PSA, TMPRSS2, keratin 8 and androgen receptor (AR) (Fig. 1h-k). The stromal markers vimentin, Thy-1 (CD90) and AR are highly expressed in the CD49f^{lo}Trop2$^-$ population (Fig. 1k-m), and the endothelial markers PECAM (CD31) and von Willebrand factor (vWF) are enriched in the CD49f^{hi}Trop2$^-$ fraction (Fig. 1n-o). Based on staining in tissue sections and expression of characteristic markers for different cell types in the human prostate, we have determined that we can

reproducibly enrich for the isolation of basal epithelial, luminal epithelial, and non-epithelial (stromal, endothelial) cell types from freshly-isolated primary human prostate tissue.

Basal and luminal fractions are not likely to be homogeneous. To determine the degree of purity for epithelial cell fractions, we performed immunohistochemical analysis on cytospins for expression of basal and luminal-specific markers. We found that almost 90% of cells from the basal fraction, but less than 0.4% of cells from the luminal fraction, express the basal-specific transcription factor p63 (Fig. 1b-c). Similarly, we found that approximately 80% of cells in the luminal fraction, but less than 0.5% of cells from the basal fraction, express the luminal differentiation marker PSA (Fig. 1b-c). We will therefore refer to the basal-enriched and luminal-enriched fractions as basal and luminal fractions respectively.

To compare the tissue-regenerative stem cell capacity of freshly-isolated basal and luminal cells, we turned to an *in vivo* prostate regeneration assay. Two recent studies have demonstrated that an epithelial-enriched preparation of dissociated fresh[11] or cultured[12] human prostate cells retain the capacity to generate phenotypically normal prostatic tubules upon transplantation *in vivo*. In our study, 10^5 primary human prostate basal or luminal cells were combined with 10^5 murine urogenital sinus mesenchyme (mUGSM) cells in Matrigel and injected subcutaneously into NOD-SCID IL2Rγ^{null} (NSG) mice, demonstrated to be permissive for growth of human cells[13]. Grafts were harvested after 6-10 weeks *in vivo* and analyzed for the presence or absence of

outgrowths. While glandular structures were absent in transplants derived from luminal cells (Fig. 2c), we found an abundance of tubules generated from prostatic basal cells (Fig. 2b). Tubules exhibit a remarkable similarity to the native architecture of the gland, demonstrated by an outer keratin 5+ basal cell layer with flat p63+ nuclei oriented parallel to the basement membrane, and a keratin 8+ luminal layer with larger AR+ nuclei oriented towards the lumen (Fig. 2d-g). Transplantation of mUGSM cells alone yields only stromal outgrowth (Fig. 2a), suggesting that possible contamination of urogenital sinus epithelium is unlikely to have contributed to gland formation. Staining for a human-specific Trop2 antibody confirms the development of human prostatic tissue (Supplementary Fig. 1). Results were reproducible for multiple independent patient samples (Fig. 2b-c) and showed little variation between replicate grafts. We observed approximately 10 tubules per graft from 10^5 sorted basal cells, demonstrating an estimated frequency similar to the mammary regenerating frequency (1/21,500) of the human mammary stem cell enriched population[14], which is identified by high levels of CD49f and EpCAM, a Trop2 family member. Therefore, the human prostate basal compartment is enriched for prostate-regenerating stem cells *in vivo*. Our results demonstrate that basal cells are capable of generating tubules consisting of both basal and luminal cells, while luminal cells are devoid of tissue-regenerative activity, suggesting an *in vivo* hierarchical relationship.

The prostate cancer cell-of-origin has been heavily debated. The expansion of a basal stem/progenitor cell type in Pten-null murine prostate cancer implicates basal cells in cancer initiation[15], and a recent study shows that Pten-null murine prostate cells with a

basal phenotype are capable of initiating PIN lesions upon transplantation[16]. Evidence also supports a luminal stem/progenitor cell in prostate cancer initiation. A population of castration-resistant luminal cells expressing the transcription factor Nkx3.1 are capable of initiating Pten-null murine prostate cancer[8]. Cell-type specific promoters can drive tumorigenesis in the mouse via site-specific genomic modification, but such transgenic approaches are not yet feasible with primary human prostate cells.

To examine the cancer-initiating activity of basal and luminal fractions, we set out to establish a direct transformation assay. Classic human epithelial transformation studies involve an initial selection process via immortalization through genetic manipulation with the SV40 T-antigen and/or the catalytic subunit of telomerase in addition to the selected oncogenes[17, 18]. A search of the literature revealed two studies in the hematopoietic system[19, 20] and none in epithelial tissues demonstrating direct transformation *in vivo* starting with an enriched subpopulation of primary human cells without prior culture adaptation or directed immortalization. To transform purified subpopulations of naïve human prostate epithelial cells, we chose oncogenic signals that are relevant to the human disease and have been previously demonstrated to transform murine prostate epithelium. Activation of the PI3K pathway is one of the most common alterations in human prostate cancer, typically via loss of PTEN, leading to activation of downstream effectors such as AKT. In murine prostate epithelium, PTEN deletion leads to the formation of PIN lesions, followed by invasive carcinoma[21], while AKT activation induces PIN lesions *in vivo*[22, 23]. Chromosomal rearrangements involving the ETS family of transcription factors

are another important class of alterations in human prostate cancer[24]. Increased expression of the ETS transcription factor ERG has been shown to promote transformation *in vivo*[5, 25, 26] and ERG over-expression can cooperate with PI3K pathway activation to accelerate this process[3-5]. Using a bicistronic lentiviral vector encoding both activated AKT and ERG[5] (Fig. 3a), we transduced 10^5 freshly-isolated basal or luminal cells and transplanted them *in vivo* with 10^5 mUGSM cells. While luminal cell-derived grafts were comprised of only stromal outgrowth (Fig. 3e, i), basal cells were capable of generating morphologically malignant structures representing varying degrees of epithelial transformation (Fig. 3b-d, f-h). We demonstrate that primary human prostate epithelial cells can be directly transformed. Our results do not differentiate between the roles of AKT and ERG in transformation. Further studies will be necessary to determine the oncogenic specificity of these and other individual genes and combinations in this assay.

Abnormal regions derived from transduced basal cells contained cells with nuclear atypia, loss of polarity, hyperchromatic nuclei, and other markers of malignant transformation (Fig. 3f-h). We observed an expansion of AR+ malignant-appearing luminal cells surrounded by a single layer of p63+ basal cells (Fig. 4a-b). In many lesions, the abnormal cells were positive for PSA as well as AR, indicating luminal differentiation. In addition, they also stained positively for AMACR (alpha-methylacyl-CoA racemase), a biomarker expressed by malignant cells of both high grade PIN and invasive prostate cancer[27] (Fig. 4c-d). Based on the presence of morphologically malignant AR+/PSA+ luminal cells that stain positively for AMACR and the retention of

a p63+ basal layer, the basal-derived lesions fulfill the histologic criteria used by pathologists for the diagnosis of high grade PIN, the precursor lesion to invasive prostate cancer[28]. High levels of membrane-bound phospho-AKT and nuclear ERG in morphologically malignant regions marked by RFP fluorescence implicate the increased expression and activation of these proteins in the formation of these lesions (Fig. 4e-h, closed arrow). Staining for a human-specific Trop2 antibody (Supplementary Fig. 1) in addition to PSA expression confirms the human origin. Although we see little response from the luminal fraction, luminal cells are capable of being infected by these lentiviruses (Supplementary Fig. 2) and persist *in vivo* long enough to respond to oncogenic stimuli (Supplementary Fig. 3). Transduction of isolated cell populations with a control lentivirus results in double-layered tubules from basal cells (Supplementary Fig. 2b) and a lack of glandular structure from luminal cells (Supplementary Fig. 2e), similar to the outgrowths from unmanipulated cell populations (Fig. 2). We observed approximately 10-20 events per graft from 10^5 sorted basal cells, reproduced among several independent patient samples, suggesting that only a subpopulation of the basal fraction can serve as target cells for transformation. Future interrogation and sub-fractionation of the basal compartment will yield a more refined target cell.

Prostate cancer is predominantly a phenotypically luminal disease, characterized by the relative absence of the basal compartment[29]. In a direct transformation assay, we now show that basal cells can generate prostate cancer-initiating lesions with luminal expansion and differentiation, as demonstrated by strong staining for AR and PSA. Together, these results suggest that the stem-like basal cells may undergo differentiation

or a loss of the basal phenotype during disease progression. While our findings do not infer that basal cells are the only cell-of-origin, we demonstrate that basal cells are an efficient target population for transformation.

In summary, we have developed a direct transformation assay that has allowed us to isolate primary human prostate basal cells with *in vivo* tissue-regenerating and cancer-initiating activity. We describe a relevant model to study human prostate tumorigenesis, enabling investigation of the genetic alterations capable of transforming benign human prostate epithelial cells, and testing of human-specific therapies that can impede initiation and progression of prostate cancer.

Methods Summary

Primary Human Cell Preparation

For tissue procurement, an approved protocol through the UCLA Office for the Protection of Research Subjects was utilized, and all human tissue samples were de-identified to protect patient confidentiality. Prostate surgical specimens were removed en bloc and an experienced technician from UCLA tissue procurement core laboratory (TPCL) prepared 5 or 6 prostatic sections approximately 3-4mm in thickness. A sleeve of fresh tissue was obtained from the posterior (peripheral zone) of selected sections. Frozen slides were prepared and stained by H&E staining. A pathologist examined slides and cancerous areas were marked and mapped to the remaining fresh tissue. Tumor nodules

were then dissected and isolated from benign tissue. The benign prostate tissue was

placed on ice, and processed as previously described[12].

References

1. Khavari, P.A. Modelling cancer in human skin tissue. *Nature Rev. Can.* **6**, 270-280 (2006).
2. Pienta, K.J. *et al.* The current state of preclinical prostate cancer animal models. *Prostate* **68**, 629-639 (2008).
3. Carver, B.S. *et al.* Aberrant ERG expression cooperates with loss of PTEN to promote cancer progression in the prostate. *Nature Gen.* **41**, 619-624 (2009).
4. King, J.C. *et al.* Cooperativity of TMPRSS2-ERG with PI3-kinase pathway activation in prostate oncogenesis. *Nature Gen.* **41**, 524-526 (2009).
5. Zong, Y. *et al.* ETS family transcription factors collaborate with alternative signaling pathways to induce carcinoma from adult murine prostate cells. *Proc. Natl Acad/ Sci. USA* **106**, 12465-12470 (2009).
6. Goldstein, A.S. *et al.* Trop2 identifies a subpopulation of murine and human prostate basal cells with stem cell characteristics. *Proc. Natl Acad/ Sci. USA* **105**, 20882-20887 (2008).
7. Lawson, D.A., Xin, L., Lukacs, R.U., Cheng, D. & Witte, O.N. Isolation and functional characterization of murine prostate stem cells. *Proc. Natl Acad/ Sci. USA* **104**, 181-186 (2007).
8. Wang, X. *et al.* A luminal epithelial stem cell that is a cell of origin for prostate cancer. *Nature* **461**, 495-500 (2009).
9. Robinson, E.J., Neal, D.E. & Collins, A.T. Basal cells are progenitors of luminal cells in primary cultures of differentiating human prostatic epithelium. *Prostate* **37**, 149-160 (1998).
10. Collins, A.T., Habib, F.K., Maitland, N.J. & Neal, D.E. Identification and isolation of human prostate epithelial stem cells based on alpha(2)beta(1)-integrin expression. *J. Cell Sci.* **114**, 3865-3872 (2001).
11. Bhatia, B. *et al.* Critical and distinct roles of p16 and telomerase in regulating the proliferative life span of normal human prostate epithelial progenitor cells. *The J. Biol. Chem.* **283**, 27957-27972 (2008).
12. Garraway, I., Sun, W., Tran, C., Perner, S., Zhang, B., Goldstein, A., Hahm, S., Haider, M., Head, C., Reiter, R., Rubin, M., Witte, O. Human prostate sphere-forming cells represent a subset of basal epithelial cells capable of glandular regeneration in vivo. *Prostate* **In Press** (2009).
13. Quintana, E. *et al.* Efficient tumour formation by single human melanoma cells. *Nature* **456**, 593-598 (2008).
14. Lim, E. *et al.* Aberrant luminal progenitors as the candidate target population for basal tumor development in BRCA1 mutation carriers. *Nature Med.* **15**, 907-913 (2009).

15. Wang, S. *et al.* Pten deletion leads to the expansion of a prostatic stem/progenitor cell subpopulation and tumor initiation. *Proc. Natl Acad. Sci. USA* **103**, 1480-1485 (2006).

16. Mulholland, D., Xin, L., Morim, A., Lawson, D., Witte, O., Wu, H. LSC Stem/Progenitors are tumor initiating cells in the Pten null prostate cancer model. *Cancer Res.* **In Press** (2009).

17. Hahn, W.C. *et al.* Creation of human tumour cells with defined genetic elements. *Nature* **400**, 464-468 (1999).

18. Elenbaas, B. *et al.* Human breast cancer cells generated by oncogenic transformation of primary mammary epithelial cells. *Genes Dev.* **15**, 50-65 (2001).

19. Barabe, F., Kennedy, J.A., Hope, K.J. & Dick, J.E. Modeling the initiation and progression of human acute leukemia in mice. *Science* **316**, 600-604 (2007).

20. Wei, J. *et al.* Microenvironment determines lineage fate in a human model of MLL-AF9 leukemia. *Cancer cell* **13**, 483-495 (2008).

21. Wang, S. *et al.* Prostate-specific deletion of the murine Pten tumor suppressor gene leads to metastatic prostate cancer. *Cancer cell* **4**, 209-221 (2003).

22. Majumder, P.K. *et al.* Prostate intraepithelial neoplasia induced by prostate restricted Akt activation: the MPAKT model. *Proc. Natl Acad. Sci. USA* **100**, 7841-7846 (2003).

23. Xin, L., Lawson, D.A. & Witte, O.N. The Sca-1 cell surface marker enriches for a prostate-regenerating cell subpopulation that can initiate prostate tumorigenesis. *Proc. Natl Acad. Sci. USA* **102**, 6942-6947 (2005).

24. Tomlins, S.A. *et al.* Recurrent fusion of TMPRSS2 and ETS transcription factor genes in prostate cancer. *Science* **310**, 644-648 (2005).

25. Klezovitch, O. *et al.* A causal role for ERG in neoplastic transformation of prostate epithelium. *Proc. Natl Acad. Sci. USA* **105**, 2105-2110 (2008).

26. Tomlins, S.A. *et al.* Role of the TMPRSS2-ERG gene fusion in prostate cancer. *Neoplasia* **10**, 177-188 (2008).

27. Wu, C.L. *et al.* Analysis of alpha-methylacyl-CoA racemase (P504S) expression in high-grade prostatic intraepithelial neoplasia. *Hum. Path.* **35**, 1008-1013 (2004).

28. McNeal, J.E. & Bostwick, D.G. Intraductal dysplasia: a premalignant lesion of the prostate. *Hum. Path.* **17**, 64-71 (1986).

29. Grisanzio, C. & Signoretti, S. p63 in prostate biology and pathology. *J. Cell. Biochem.* **103**, 1354-1368 (2008).

30. Xin, L., Ide, H., Kim, Y., Dubey, P. & Witte, O.N. In vivo regeneration of murine prostate from dissociated cell populations of postnatal epithelia and urogenital sinus mesenchyme. *Proc. Natl Acad. Sci. USA* **100 Suppl 1**, 11896-11903 (2003).

Author Contributions

A.S.G. performed experiments. J.H. provided pathologic analysis and performed immunohistochemical stains. C.G. processed tissue. A.S.G., J.H., I.P.G. and O.N.W. designed and analyzed research. A.S.G. and O.N.W. wrote the paper.

Figure Legends

Figure 1. Purification of basal and luminal epithelial cells from freshly-isolated human prostate tissue. a, FACS plot shows the distribution of dissociated primary prostate cells based on expression of CD49f and Trop2 and gates drawn to distinguish four populations. **b**, Immunostaining of FACS-purified CD49f^{hi}Trop2^{hi} (basal) and CD49f^{lo}Trop2^{hi} (luminal) fractions for p63 or PSA (red) and counterstained with DAPI (blue). Scale bar, 100 μm and 17 μm (inset). **c**, Percentages (mean +/- s.d. for three

independent patients) of FACS-purified basal and luminal cells that stain positively for p63 or PSA. **d**, Proposed identity of each cell population based on differential expression of CD49f and Trop2 and color coding used for e-o. **e-o**, Quantitative real-time PCR analysis of transcript levels in different subpopulations (mean +/- s.d. for two independent patient samples compared to total unfractionated prostate cells, set at 1).

Figure 2. Basal cells have human prostate-regenerating activity *in vivo*. a-c, Outgrowths generated from dissociated cells transplanted subcutaneously into NSG mice. Representative images shown from experiments reproduced using independent patient samples. Scale bars, 100 μm **a**, mUGSM cells transplanted alone generate only stromal outgrowth. **b**, Basal cells combined with mUGSM cells generate glandular structures. **c**, Luminal cells combined with mUGSM cells fail to generate glandular structures. **d-f**, High power images of immunostained prostatic tubules generated from basal cells. Scale bars, 20 μm. **d-e**, Tubules contain an outer layer of p63+ basal cells (d) and an inner layer of AR+ luminal cells (e). **f-g**, Co-stained images demonstrate distinct basal and luminal layers with DAPI nuclear counterstain (blue). **f**, Flat p63+ basal nuclei (red) surrounding larger AR+ luminal nuclei (green). Yellow spots are negative for DAPI and indicate auto-fluorescent spots rather then nuclei. **g**, Keratin 5 (green) in basal cells and keratin 8 (red) in luminal cells.

Figure 3. Direct transformation of primary human prostate epithelial cells. a, Schematic of lentiviral vector used to transduce primary prostate cells encoding oncogenes AKT and ERG in addition to the fluorescent marker RFP. **b-d**, Haematoxylin

and eosin (H&E) stained sections of transformed epithelial structures derived from transduced basal cells. Scale bars, 200 μm. **e**, H&E section with a lack of epithelial structure from transduced luminal cells. Scale bar, 200 μm. **f-i**, High-power images of boxed regions from b-e. Scale bars, 50 μm. Representative images from experiments reproduced using independent patient samples.

Figure 4. Transformed lesions resemble high grade PIN. a-b, Immunohistochemical staining for luminal (a) and basal (b) cells within transformed structures shows luminal expansion with retention of the basal layer. Scale bars, 100 μm. **c-d**, Cytoplasmic staining for PSA (c) and AMACR (d) within transformed structures. Scale bars, 50 μm. **e-h**, Serial sections of a transformed structure (closed arrow) next to a benign tubule (open arrow). Scale bars, 100 μm. **e**, H&E stain. **f-h,** High levels of expression of RFP (f, red), membrane-bound phospho-AKT (g, brown), and nuclear ERG (h, green) in the abnormal structure (closed arrow) but not in the neighboring benign tubule (open arrow).

Full Methods

Cell Separation

Dissociated cells were stained with primary antibodies: PE or Alexa Fluor 647-conjugated CD49f (Clone GoH3, BioLegend) and biotinylated Trop2 (BAF650, R&D Systems) for 15 minutes on ice, followed by staining with secondary antibody: Streptavidin conjugated to APC or APC-Cy7 (BioLegend) for 15 minutes on ice. Cells are stained in fully-supplemented PrEGM (Clonetics) in addition to 2.5 μg/ml Fungizone

(Gibco) and 10 μm of the p160ROCK inhibitor Y-27632 dihydrochloride (Tocris Bioscience). Sorting was performed on the BD FACS Aria II (BD Biosciences).

Lentiviral transduction and *in vivo* assays

Lentiviral vector construction, preparation, and titering were previously described[5]. FACS-purified cells were counted by hemacytometer, and spinduction was carried out as described[30]. Lentivirally transduced cells were washed three times with PBS, combined with mUGSM cells, pelleted and resuspended in 30 μl cold Matrigel (BD Biosciences) and kept on ice. Cell/Matrigel mixtures were injected subcutaneously into NSG mice (NOD-SCID-IL2Rγ[null], originally purchased from The Jackson Laboratory and housed and bred under the regulation of the Division of Laboratory Animal Medicine at UCLA). Grafts were harvested 6-10 weeks later and subjected to further analysis.
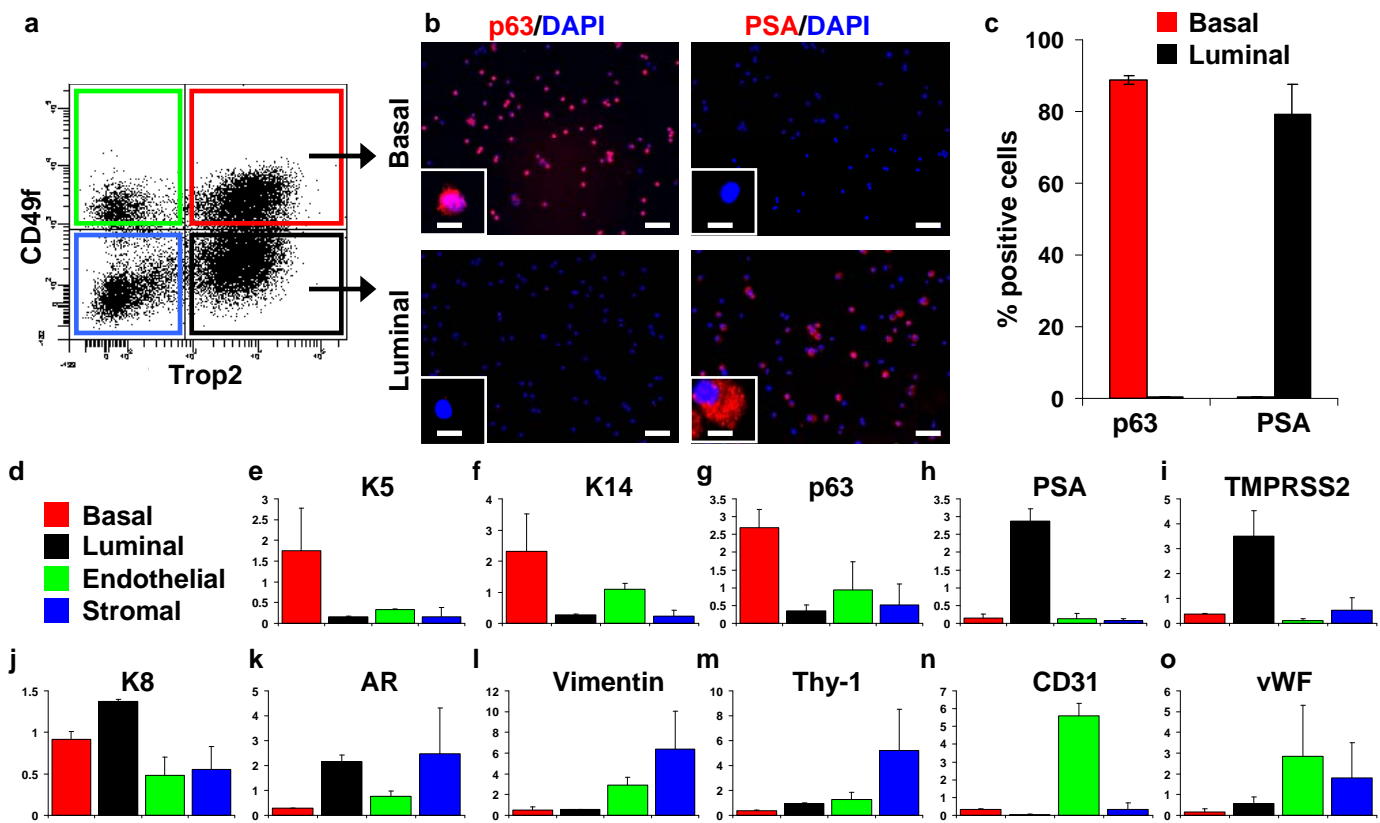
Immunohistochemical and Immunofluorescent analysis

Paraffin-embedded tissue was analyzed as previously described[7, 30] . Primary antibodies used: p63 (Santa Cruz, sc-8431), AR (Santa Cruz, sc-816), Keratin 5 (Covance, PRB-160P), Keratin 8 (Covance, MMS-162P), Trop2 (R&D, BAF650), PSA (DAKO, A0562), AMACR (DAKO, M3616), pAKT (Cell Signaling, 3787), ERG (Santa Cruz, sc-353). Secondary antibodies used: Streptavidin-fluorescein, Goat-anti-mouse IgG conjugated to Alexa Fluor 594 or Alexa Fluor 488, Goat-anti-Rabbit IgG conjugated to Alexa Fluor 594 or Alexa Fluor 488 (all from Invitrogen/Molecular Probes). For cytospins, 10,000 FACS-purified cells were spun down onto glass slides as previously described[7].
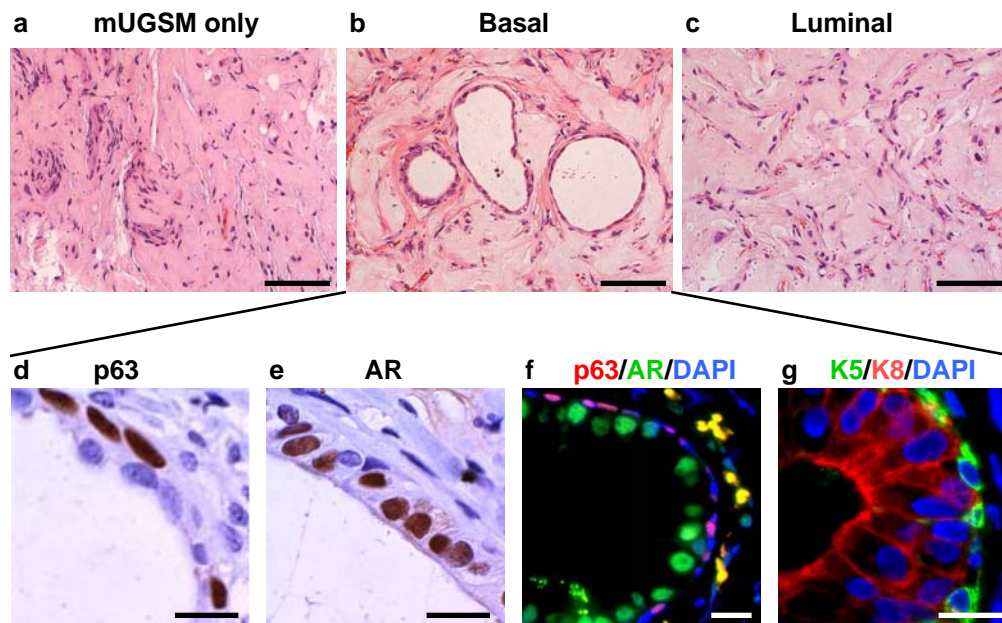
RNA Isolation and Quantitative Reverse Transcription-Polymerase Chain Reaction

Total RNA was isolated from FACS-isolated prostate populations using the RNEasy Micro Kit (Qiagen) and reverse transcription was carried out using SuperScript III first-strand synthesis system (Invitrogen). qRT-PCR and subsequent analysis was performed using the iQ SYBR Green Supermix for Real-Time PCR (Bio-Rad) on a Bio-Rad iCycler and iQ5 2.0 Standard Edition Optical System Software. Data was analyzed using the Pfaffl method. Target gene expression was normalized to human GAPDH. Primer sequences are listed below. Commercial primers for p63, PSA, TMPRSS2, AR, Thy-1 and vWF were purchased from SA Biosciences.
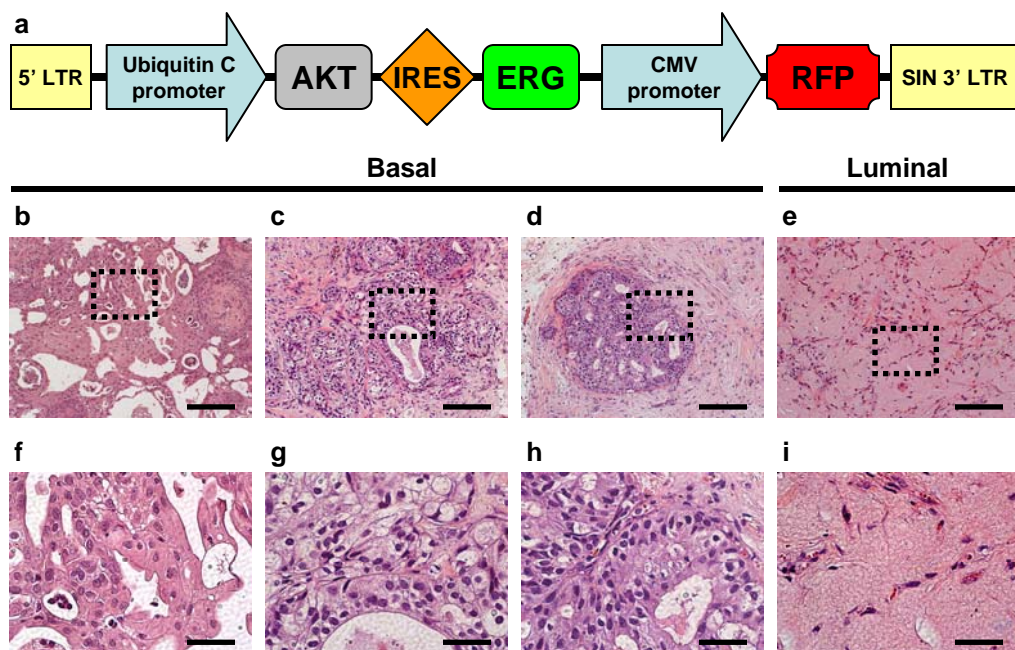
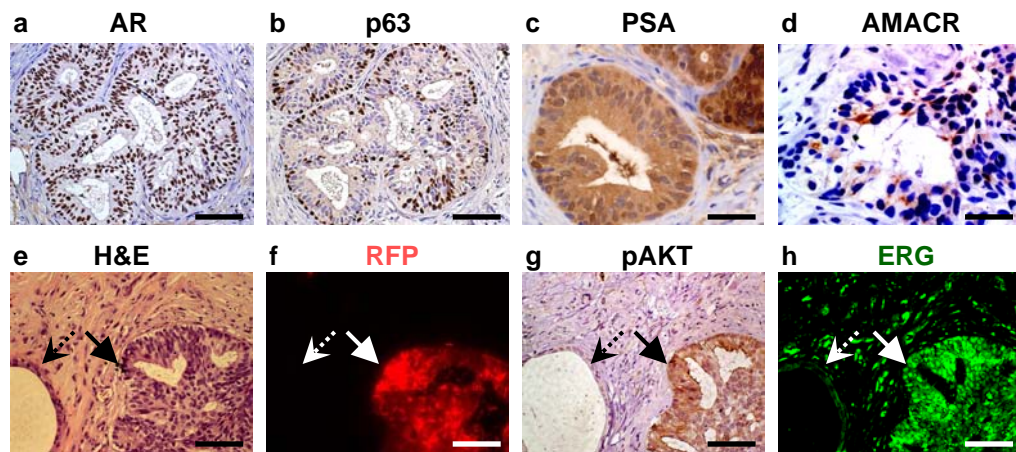| Gene	5' primer	3' primer
GAPDH:	CTCTCTGCTCCTCCTGTTCGAC	TGAGCGATGTGGCTCGGCT
Keratin 5:	CTGGTCCAACTCCTTCTCCA	GGAGCTCATGAACACCAAGC
Keratin 14:	GACCATTGAGGACCTGAGGA	ATTGATGTCGGCTTCCACAC
K8:	TGCAGAACATGAGCATTC	CAGAGGATTAGGGCTGAT
Vimentin:	GCAAAGATTCCACTTTGCGT	GAAATTGCAGGAGGAGATGC
CD31:	GGGTCAGGTTCTTCCCATTT	CCTTCTGCTCTGTTCAAGCC

Witte (Goldstein *et al.*), Fig. 1, 183 mm wide x 110 mm high

a   mUGSM only   b   Basal   c   Luminal

d   p63   e   AR   f   p63/AR/DAPI   g   K5/K8/DAPI

Witte (Goldstein *et al.*), Fig. 2, 136 mm wide x 85 mm high

a

| 5' LTR | Ubiquitin C promoter | AKT | IRES | ERG | CMV promoter | RFP | SIN 3' LTR |

Basal **Luminal**

b **c** **d** **e**

f **g** **h** **i**

Witte (Goldstein *et al.*), Fig. 3, 136 mm wide x 89 mm high

a   AR   b   p63   c   PSA   d   AMACR

e   H&E   f   RFP   g   pAKT   h   ERG

Witte (Goldstein *et al.*), Fig. 4, 136 mm wide x 62 mm high

a   Mouse prostate   **b**   Human basal + FUCRW   **c**   Human basal + AKT-IRES-ERG

d   Mouse UGSM   **e**   Human luminal + FUCRW   **f**   Human luminal + AKT-IRES-ERG
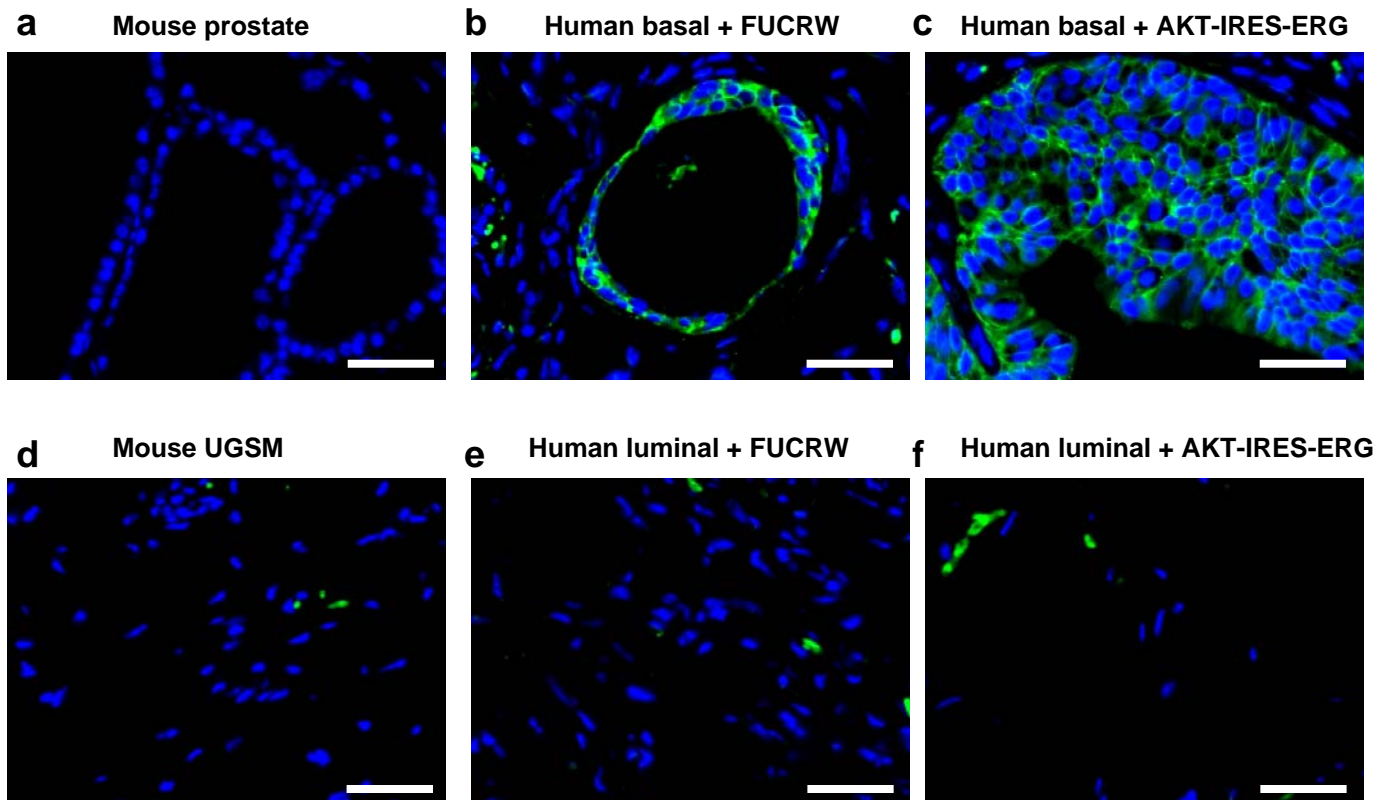
Supplementary Fig. 1. Staining of human-specific Trop2 antibody confirms human identity of regenerated tissue structures. Immunostaining for human Trop2 (green) with DAPI nuclear counterstain (blue) on paraffin-embedded regenerated tissue from mouse prostate cells (a, negative control), human prostate basal cells transduced with control FUCRW (b) or AKT-IRES-ERG lentivirus (c), human prostate luminal cells transduced with control FUCRW (e) or AKT-IRES-ERG lentivirus (f). Regenerated tissue from mouse UGSM cells alone also serves as a negative control for the expression of human-specific Trop2. (d). Scale bars, 50 μm.

a

FACS sort basal and luminal cells → Spinfection with FUCRW (RFP) lentivirus → Plate cells in vitro for 48 hours → Analyze for RFP expression

FACS sort basal and luminal cells → Spinfection with no lentivirus → Plate cells in vitro for 48 hours → Analyze for RFP expression

b Basal no infection

0.1%

SSC-A (× 1,000)
RFP PE-Texas Red-A

c Basal RFP infection

11.2%

SSC-A (× 1,000)
RFP PE-Texas Red-A

d Luminal no infection

0.1%

SSC-A (× 1,000)
RFP PE-Texas Red-A

e Luminal RFP infection

7.8%

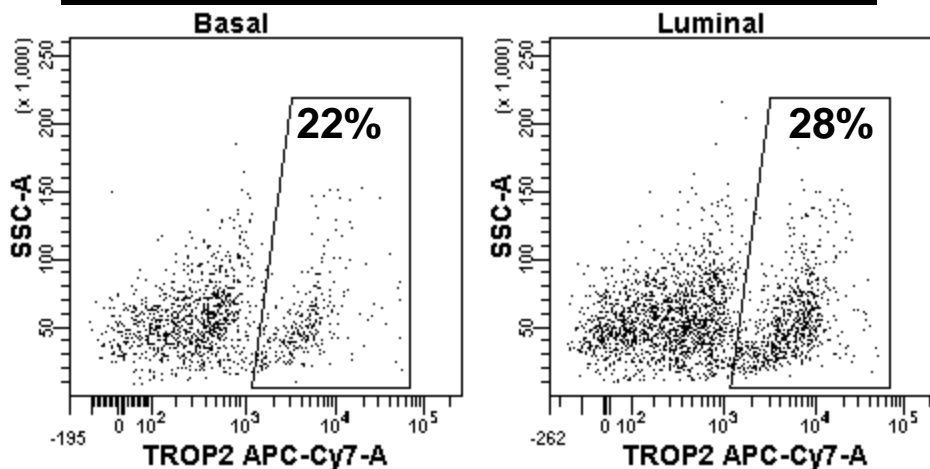SSC-A (× 1,000)
RFP PE-Texas Red-A

Supplementary Fig. 2. Human prostate basal and luminal cells are capable of lentiviral transduction. Freshly-isolated human prostate cells were sorted by FACS. 100,000 human prostate basal or luminal cells were transduced with FUCRW (RFP-containing) control lentivirus, or mock infected, and cells were plated in vitro for 48 hours. Cells were grown in serum-free PrEGM media (fully supplemented). After 48 hours, RFP expression was assessed using the mock infected cells to set the gate. Both basal and luminal cells show infection with RFP after 48 hours.

Purity check after FACS sort
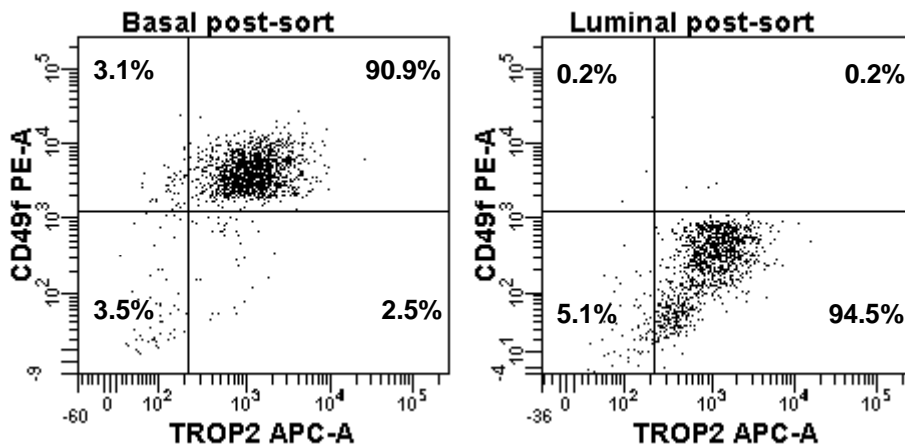
4 days after transplantation

Supplementary Fig. 3. Human prostate basal and luminal cells persist in grafts 4 days after transplantation. Freshly-isolated human prostate cells were sorted by FAC S. Post-sort analysi s demonstrates greater than 90% purity for basal and luminal fr actions. 100,000 basal or luminal cells were combined with 100,000 mUGSM cells in Matrigel and implanted *in vivo* in NSG mice. After four days, animals were sacrificed and grafts were harvested. Grafts were dissociated to single cells using subsequent digests with collagenase and trypsin as described for normal prostate tissue dissociation. Cells were stained for Trop2. Tissue derived from basal and luminal cells both show evidence of human epithelial cells persisting in grafts as demonstrated by the positive gate.